Jets in the BFKL approach and beyond

Samuel Wallon

Sorbonne Université

and

Laboratoire de Physique Théorique

CNRS / Université Paris Sud

Orsay

Towards accuracy at small x

Higgs Centre for Theoretical Physics

12 September 2019

based on works with:

R. Boussarie, D. Colferai, B. Ducloué, A. V. Grabovsky, D. Yu. Ivanov, A. H. Mueller, F. Schwennsen, L. Szymanowski, B.-W. Xiao, F. Yuan

Mueller-Navelet jets in a nutshell

Mueller-Navelet jets (1987) at $pp(\bar{p})$ colliders

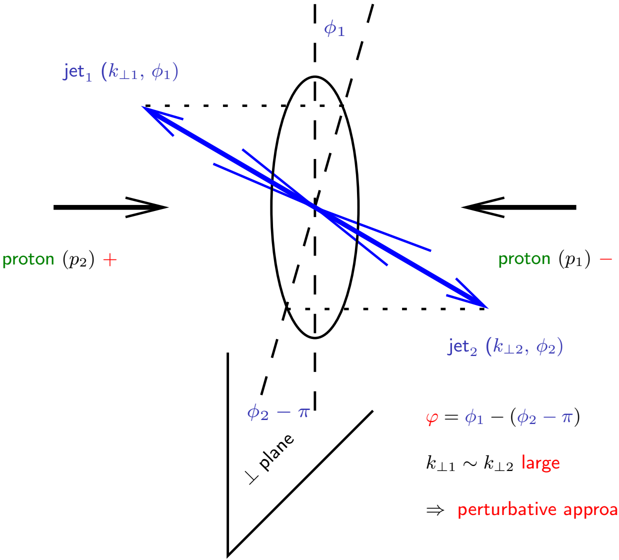

$\varphi = \phi_1 - (\phi_2 - \pi)$

$k_{\perp 1} \sim k_{\perp 2}$ large

$\Rightarrow$ perturbative approach

Mueller-Navelet jets in a nutshell

Mueller-Navelet jets (1987) at $pp(\bar{p})$ colliders

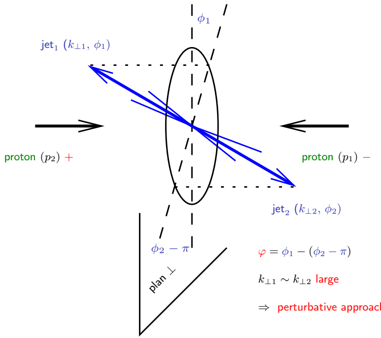

$\varphi = \phi_1 - (\phi_2 - \pi)$

$k_{\perp 1} \sim k_{\perp 2}$ large

$\Rightarrow$ perturbative approach

lowest order

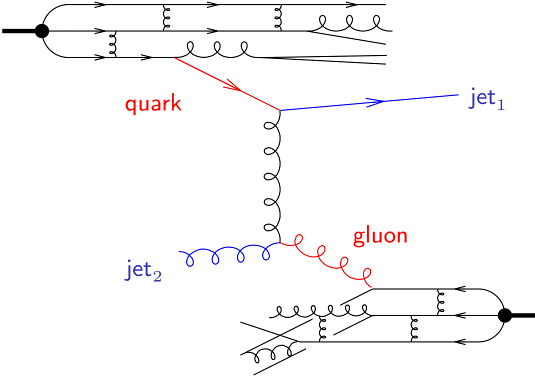

$\varphi = 0$

Mueller-Navelet jets in a nutshell

Mueller-Navelet jets (1987) at $pp(\bar{p})$ colliders

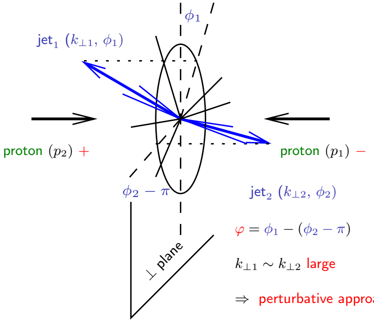

$\varphi = \phi_1 - (\phi_2 - \pi)$

$k_{\perp 1} \sim k_{\perp 2}$ large

$\Rightarrow$ perturbative approach

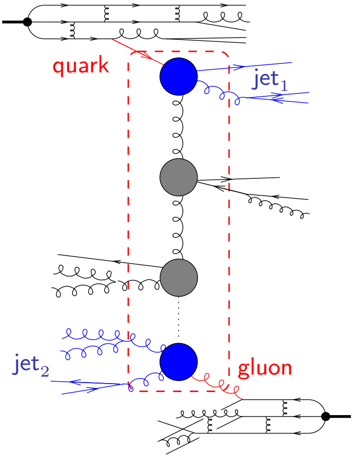

LHC: very high available energy!

emitting a lot of semi-hard partons cost very few energy

$\Rightarrow$ large cross-section + decorrelation (from overall momentum conservation)

thus $\varphi \neq 0$

References

BFKL approach

- *Mueller Navelet jets at LHC - complete NLL BFKL calculation*,
  D. Colferai, F. Schwennsen, L. Szymanowski, *S. W.*,
  JHEP **1012** (2010) 026 [arXiv:1002.1365 [hep-ph]]
- *Confronting Mueller-Navelet jets in NLL BFKL with LHC experiments at 7 TeV*,
  B. Ducloué, L. Szymanowski, *S. W.*,
  JHEP **1305** (2013) 096 [arXiv:1302.7012 [hep-ph]]
- *Evidence for high-energy resummation effects in Mueller-Navelet jets at the LHC*,
  B. Ducloué, L. Szymanowski, *S. W.*,
  Phys. Rev. Lett. **112** (2014) 082003 [arXiv:1309.3229 [hep-ph]]
- *Violation of energy-momentum conservation in Mueller-Navelet jets production*,
  B. Ducloué, L. Szymanowski, *S. W.*,
  Phys. Lett. B738 (2014) 311-316 [arXiv:1407.6593 [hep-ph]]
- *Evaluating the double parton scattering contribution to Mueller-Navelet jets production at the LHC*,
  B. Ducloué, L. Szymanowski, *S. W.*,
  Phys. Rev. D92 (2015) 7, 076002 [arXiv:1507.04735 [hep-ph]]
- *Sudakov Resummations in Mueller-Navelet Dijet Production*,
  A. H. Mueller, L. Szymanowski, *S. W.*, B.-W. Xiao, F. Yuan,
  JHEP 1603 (2016) 096 [arXiv:1512.07127 [hep-ph]]
- *Forward J/Ψ and very backward jet inclusive production at the LHC*,
  R. Boussarie, B. Ducloué, L. Szymanowski, *S. W.*,
  Phys. Rev. D97 (2018) 014008 [arXiv:1709.01380 [hep-ph]]

References

Beyond BFKL: QCD shockwave approach

[backup]

- *Impact factor for high-energy two and three jets diffractive production*,
  R. Boussarie, A. V. Grabovsky, L. Szymanowski, *S. W.*,
  JHEP **1409** (2014) 026 [arXiv:1405.7676 [hep-ph]]
- *On the one loop $\gamma^{(*)} \to q\bar{q}$ impact factor and the exclusive diffractive cross sections for the production of two or three jets*,
  R. Boussarie, A. V. Grabovsky, L. Szymanowski, *S. W.*,
  JHEP **1611** (2016) 149 [arXiv:1606.00419 [hep-ph]]
- *Next-to-Leading Order Computation of Exclusive Diffractive Light Vector Meson Production in a Saturation Framework*,
  R. Boussarie, A. V. Grabovsky, D. Yu. Ivanov, L. Szymanowski, *S. W.*,
  Phys. Rev. Lett. **119** (2017) 072002 [arXiv:1612.08026 [hep-ph]]
- *Towards a complete next-to-logarithmic description of forward exclusive diffractive dijet electroproduction at HERA: real corrections*,
  R. Boussarie, A. V. Grabovsky, L. Szymanowski, *S. W.*,
  to appear in PRD [arXiv:1905.07371 [hep-ph]]

DIS

The various regimes governing the perturbative content of the proton

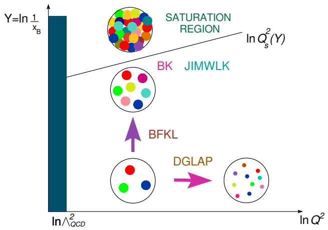

- "usual" regime: x_B moderate ($x_B \gtrsim .01$):
  Evolution in Q governed by the QCD renormalization group
  (Dokshitser, Gribov, Lipatov, Altarelli, Parisi equation)

$$\underbrace{\sum_n (\alpha_s \ln Q^2)^n}_{\text{LLQ}} + \underbrace{\alpha_s \sum_n (\alpha_s \ln Q^2)^n}_{\text{NLLQ}} + \cdots$$

- perturbative Regge limit: $s_{\gamma^* p} \to \infty$ i.e. $x_B \sim Q^2/s_{\gamma^* p} \to 0$
  in the perturbative regime (hard scale Q^2)
  (Balitski Fadin Kuraev Lipatov equation)

$$\underbrace{\sum_n (\alpha_s \ln s)^n}_{\text{LLs}} + \underbrace{\alpha_s \sum_n (\alpha_s \ln s)^n}_{\text{NLLs}} + \cdots$$

QCD in the perturbative Regge limit

- One of the important longstanding theoretical questions raised by QCD is its behaviour in the perturbative Regge limit $s \gg -t$
- Based on theoretical grounds, one should identify and test suitable observables in order to test this peculiar dynamics

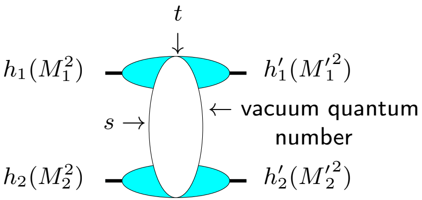

hard scales: $M_1^2,\ M_2^2 \gg \Lambda^2_{QCD}$ or $M'^2_1,\ M'^2_2 \gg \Lambda^2_{QCD}$ or $t \gg \Lambda^2_{QCD}$
where the $t-$channel exchanged state is the so-called hard Pomeron

How to test QCD in the perturbative Regge limit?

What kind of observable?

- perturbation theory should be applicable:
  selecting external or internal probes with transverse sizes $\ll 1/\Lambda_{QCD}$ (*hard* γ^*, *heavy* meson (J/Ψ, Υ), *energetic* forward jets) or by choosing large t in order to provide the hard scale.

- governed by the *"soft"* perturbative dynamics of QCD

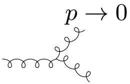

and *not* by its *collinear* dynamics

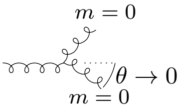

$\Longrightarrow$ select semi-hard processes with $s \gg p_{T\,i}^2 \gg \Lambda_{QCD}^2$ where $p_{T\,i}^2$ are typical transverse scale, all of the same order.

How to test QCD in the perturbative Regge limit?

Some examples of processes

- inclusive: DIS (HERA), diffractive DIS, total $\gamma^*\gamma^*$ cross-section (LEP, ILC)
- semi-inclusive: forward jet and π^0 production in DIS, Mueller-Navelet double jets, diffractive double jets, high p_T central jet, dihadron production in hadron-hadron colliders (Tevatron, LHC), inclusive photoproduction of two heavy quark-antiquark pairs at e^+e^- colliders (ILC)
- exclusive: exclusive meson production in DIS, double diffractive meson production at e^+e^- colliders (ILC), ultraperipheral events at LHC ($\mathbb{P}$omeron, $\mathbb{O}$dderon)

Resummation in QCD: DGLAP vs BFKL

Small values of α_s (perturbation theory applies if there is a hard scale) can be compensated by large logarithmic enhancements.

DGLAP

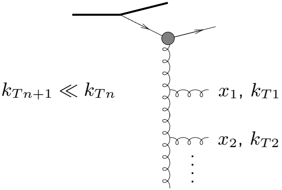

strong ordering in k_T

$$\sum(\alpha_s \ln Q^2)^n$$

BFKL

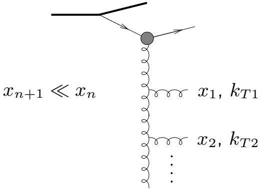

strong ordering in x

$$\sum(\alpha_s \ln s)^n$$

When $\sqrt{s}$ becomes very large, it is expected that a BFKL description is needed to get accurate predictions

The specific case of QCD at large s

QCD in the perturbative Regge limit

The amplitude can be written as:

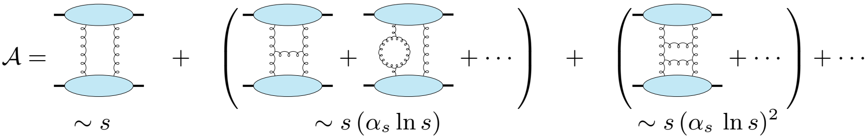

this can be put in the following form :

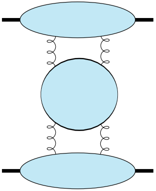

$\leftarrow$ Impact factor

$\leftarrow$ Green's function

$\leftarrow$ Impact factor

$$\sigma_{tot}^{h_1\, h_2 \to anything} = \frac{1}{s} Im\mathcal{A} \sim s^{\alpha_{\mathbb{P}}(0)-1}$$

with $\alpha_{\mathbb{P}}(0) - 1 = C\,\alpha_s + C'\,\alpha_s^2 + \cdots$

$C > 0$: Leading Log $\mathbb{P}$omeron

Balitsky, Fadin, Kuraev, Lipatov

Opening the boxes: Impact representation $\gamma^* \gamma^* \to \gamma^* \gamma^*$ as an example

- Sudakov decomposition: $k_i = \alpha_i\, p_1 + \beta_i\, p_2 + k_{\perp i}$ $\quad (p_1^2 = p_2^2 = 0,\ 2p_1 \cdot p_2 = s)$
- write $\quad d^4 k_i = \frac{s}{2}\, d\alpha_i\, d\beta_i\, d^2 k_{\perp i}$ $\quad$ ($\underline{k}$ = Eucl. $\leftrightarrow$ $k_\perp$ = Mink.)
- $t-$channel gluons have non-sense polarizations at large s: $\epsilon_{NS}^{up/down} = \frac{2}{s}\, p_{2/1}$

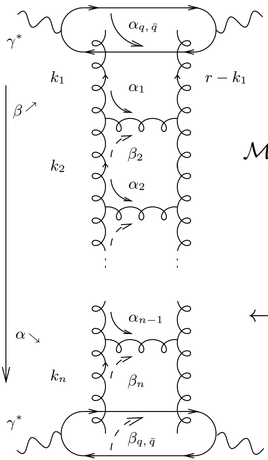

$\Rightarrow$ set $\alpha_1 = 0$ and $\int d\beta_1 \;\Rightarrow\; \Phi^{\gamma^* \to \gamma^*}(\underline{k}_1, \underline{r} - \underline{k}_1)$

impact factor

$$\mathcal{M} = \frac{is}{(2\pi)^2} \int \frac{d^2\underline{k}}{\underline{k}^2}\, \Phi^{up}(\underline{k},\, \underline{r} - \underline{k}) \int \frac{d^2\underline{k}'}{\underline{k}'^2}\, \Phi^{down}(-\underline{k}',\, -\underline{r} + \underline{k}')$$
$$\times \int_{\delta - i\infty}^{\delta + i\infty} \frac{d\omega}{2\pi i} \left(\frac{s}{s_0}\right)^{\omega} G_\omega(\underline{k}, \underline{k}', \underline{r})$$

$\longleftarrow$ multi-Regge kinematics

$\Rightarrow$ set $\beta_n = 0$ and $\int d\alpha_n \;\Rightarrow\; \Phi^{\gamma^* \to \gamma^*}(-\underline{k}_n, -\underline{r} + \underline{k}_n)$

Higher order corrections

- Higher order corrections to BFKL kernel are known at NLL order (Lipatov Fadin; Camici, Ciafaloni), now for arbitrary impact parameter $\alpha_S \sum_n (\alpha_S \ln s)^n$ resummation

- impact factors are known in some cases at NLL
  - $\gamma^* \to \gamma^*$ at $t = 0$ (Bartels, Colferai, Gieseke, Kyrieleis, Qiao; Balitski, Chirilli)
  - forward jet production (Bartels, Colferai, Vacca; Caporale, Ivanov, Murdaca, Papa, Perri; Chachamis, Hentschinski, Madrigal, Sabio Vera)
  - inclusive production of a hadron (Ivanov, Papa)
  - $\gamma_L^* \to \rho_L$ in the forward limit (Ivanov, Kotsky, Papa)

Mueller-Navelet jets: Basics

Mueller-Navelet jets

- Consider two jets (hadrons flying within a narrow cone) separated by a large rapidity, i.e. each of them almost fly in the direction of the hadron “close“ to it, and with very similar transverse momenta
- Pure LO *collinear* treatment: these two jets should be emitted back to back at leading order:
  - $\varphi \equiv \Delta\phi - \pi = 0$ ($\Delta\phi = \phi_1 - \phi_2 =$ relative azimuthal angle)
  - $k_{\perp 1}$=$k_{\perp 2}$. No phase space for (untagged) multiple (DGLAP) emission between them

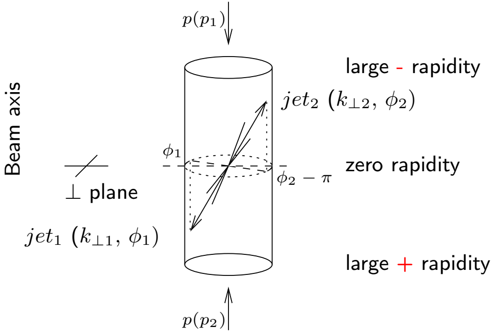

A long story

- dijets with large rapidity separation as a probe of BFKL resummation effects: A. H. Mueller, H. Navelet 1987

  BFKL LL: cross-sections

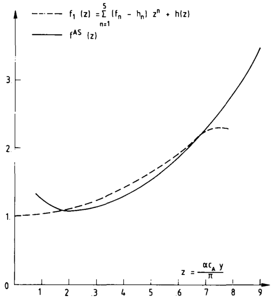

idea: study the ratio $\frac{\sigma(s_1)}{\sigma(s_2)}$
for two different values of s_1 and s_2
with fixed values of $x_{J,1}$, $x_{J,2}$
$\Rightarrow$ access to the Pomeron trajectory
(LL argument: PDFs simplifies)

note: LHC: $z \simeq 1$
$\Rightarrow$ one should not use any saddle point approximation when evaluating the BFKL Green's function

- BFKL LL: cross-section + azimuthal decorrelation
  V. Del Duca and C.R. Schmidt; W. Stirling 1994

A long story

- modified BFKL LL:
  - MC event generator: energy-momentum conservation + running of alpha
    L. Orr, W. Stirling 1997
    J. R. Andersen, V. Del Duca, S. Frixione, C. R. Schmidt, W. J. Stirling 2001
    note: the balanced situation ($k_{TJ1}^{min} = k_{TJ2}^{min}$) was shown to be problematic, calling for a resummation of Sudakov-type logs
  - kinematical constraint along the parton chain:
    J. Kwiecinski, A. D. Martin, L. Motyka and J. Outhwaite 2001
- mixed: NLL BFKL Green function + LL jet vertex
  A. Sabio Vera, F. Schwennsen; C. Marquet, C. Royon 2007
- Full NLL BFKL
  our group 2010...
  and then 2013...
  F. Caporale, G. Chachamis, F. Celiberto, D. Gordo Gómez, D. Yu. Ivanov, B. Murdaca, A. Papa, A. Sabio Vera, C. Salas
- see also HEJ (based on the Multi-Regge Kinematics (MRK) à la LL BFKL) which goes beyond LL BFKL) 2011...
  J. R. Andersen, L. Lönnblad, J. M. Smillie

Mueller-Navelet jets at LL fails

Mueller Navelet jets at LL BFKL

- in LL BFKL ($\sim \sum(\alpha_s \ln s)^n$), emission between these jets $\longrightarrow$ strong decorrelation between the relative azimutal angle jets, incompatible with $p\bar{p}$ Tevatron collider data
- a collinear treatment at next-to-leading order (NLO) can describe the data
- important issue: non-conservation of energy-momentum along the BFKL ladder. A LL BFKL-based Monte Carlo combined with e-m conservation improves dramatically the situation (Orr and Stirling)

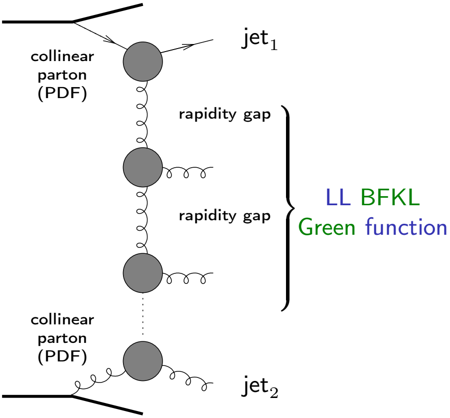

Multi-Regge kinematics (LL BFKL)

Studies at LHC: Mueller-Navelet jets

Mueller Navelet jets at NLL BFKL

- up to now, the subseries $\alpha_s \sum (\alpha_s \ln s)^n$ NLL was included only in the exchanged $\mathbb{P}$omeron state, and not inside the jet vertices
  Sabio Vera, Schwennsen
  Marquet, Royon
- the common belief was that these corrections should not be important

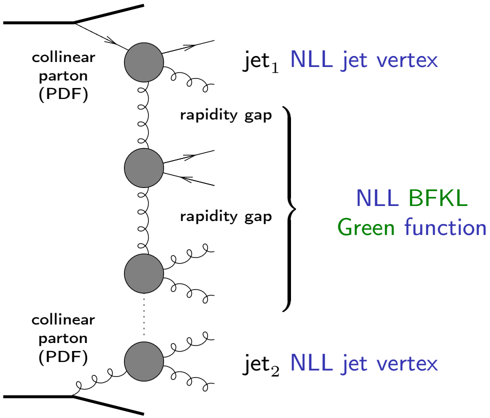

Quasi Multi-Regge kinematics (here for NLL BFKL)

Jet vertex: LL versus NLL

$\mathbf{k}, \mathbf{k}' =$ Euclidian two dimensional vectors

LL jet vertex:

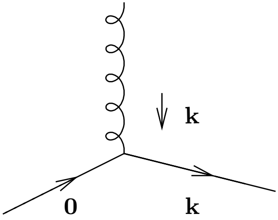

NLL jet vertex:

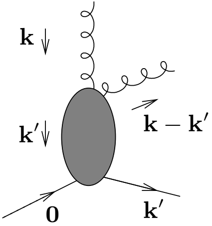

Jet vertex: jet algorithms

Jet algorithms

- a jet algorithm should be IR safe, both for soft and collinear singularities
- the most common jet algorithm are:
  - cone algorithm (not IR safe in general; can be made IR safe at NLO: Ellis, Kunszt, Soper)
  - k_t and anti-k_t algorithms (IR safe)

Jet vertex: cone jet algorithms

Cone jet algorithm at NLO (Ellis, Kunszt, Soper)

- Should partons $(|\mathbf{p}_1|, \phi_1, y_1)$ and $(\mathbf{p}_2|, \phi_2, y_2)$ combined in a single jet? $|\mathbf{p}_i|$ =transverse energy deposit in the calorimeter cell i of parameter $\Omega = (y_i, \phi_i)$ in $y - \phi$ plane
- define transverse energy of the jet: $p_J = |\mathbf{p}_1| + |\mathbf{p}_2|$
- jet axis:

$$\Omega_c \begin{cases} y_J = \dfrac{|\mathbf{p}_1|\, y_1 + |\mathbf{p}_2|\, y_2}{p_J} \\[2ex] \phi_J = \dfrac{|\mathbf{p}_1|\, \phi_1 + |\mathbf{p}_2|\, \phi_2}{p_J} \end{cases}$$

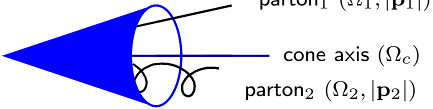

$\Omega = (y_i, \phi_i)$ in $y - \phi$ plane

If distances $|\Omega_i - \Omega_c|^2 \equiv (y_i - y_c)^2 + (\phi_i - \phi_c)^2 < R^2$ $(i = 1$ and $i = 2)$

$\Longrightarrow$ partons 1 and 2 are in the same cone Ω_c

combined condition: $|\Omega_1 - \Omega_2| < \dfrac{|\mathbf{p}_1| + |\mathbf{p}_2|}{max(|\mathbf{p}_1|, |\mathbf{p}_2|)} R$

Jet vertex: LL versus NLL and cone jet algorithm

LL jet vertex and cone algorithm

$\mathbf{k}, \mathbf{k}'$ = Euclidian two dimensional vectors

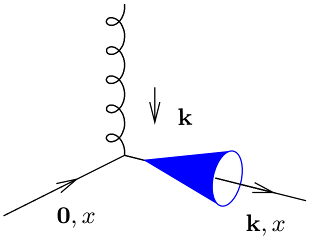

$$\mathcal{S}_J^{(2)}(k_\perp; x) = \delta\left(1 - \frac{x_J}{x}\right) |\mathbf{k}|\, \delta^{(2)}(\mathbf{k} - \mathbf{k}_J)$$

Jet vertex: LL versus NLL and cone jet algorithm

NLL jet vertex and cone algorithm

$\mathbf{k}, \mathbf{k}'$ = Euclidian two dimensional vectors

$$\mathcal{S}_J^{(3,\mathrm{cone})}(\mathbf{k}', \mathbf{k}-\mathbf{k}', xz; x) =$$

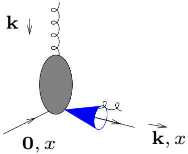

$$\mathcal{S}_J^{(2)}(\mathbf{k}, x)\, \Theta\left(\left[\frac{|\mathbf{k}-\mathbf{k}'|+|\mathbf{k}'|}{\max(|\mathbf{k}-\mathbf{k}'|,|\mathbf{k}'|)} R_{\mathrm{cone}}\right]^2 - \left[\Delta y^2 + \Delta\phi^2\right]\right)$$

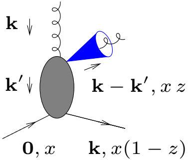

$$+\, \mathcal{S}_J^{(2)}(\mathbf{k}-\mathbf{k}', xz)\, \Theta\left(\left[\Delta y^2 + \Delta\phi^2\right] - \left[\frac{|\mathbf{k}-\mathbf{k}'|+|\mathbf{k}'|}{\max(|\mathbf{k}-\mathbf{k}'|,|\mathbf{k}'|)} R_{\mathrm{cone}}\right]^2\right)$$

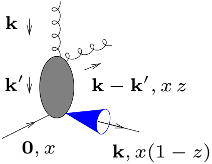

$$+\, \mathcal{S}_J^{(2)}(\mathbf{k}', x(1-z))\, \Theta\left(\left[\Delta y^2 + \Delta\phi^2\right] - \left[\frac{|\mathbf{k}-\mathbf{k}'|+|\mathbf{k}'|}{\max(|\mathbf{k}-\mathbf{k}'|,|\mathbf{k}'|)} R_{\mathrm{cone}}\right]^2\right),$$

Jet vertex: k_T and anti-k_T jet algorithms

k_T algorithm (Cacciari, Salam, Soyez)

$$\begin{aligned} d_{ij} &= \min\left(p_i^2, p_j^2\right) \frac{(y_i - y_j)^2 + (\phi_i - \phi_j)^2}{R_{k_t}^2} \\ d_{iB} &= p_i^2 \end{aligned}$$

R_{k_t} = size parameter of the jet

- identify the smallest d_{ij}, d_{iB}
- if it is a d_{ij} combine i and j
- if it is a d_{iB}, i is considered as a jet
- this is done until all the particles are clustered into jets

At NLO, there are 3 distances to be computed: d_{12}, d_{1B} and d_{2B}.
Condition for particles 1 and 2 to be combined into a jet:

$$d_{12} < d_{2b}, d_{1b} \Leftrightarrow \Delta y^2 + \Delta\phi^2 < R_{k_t}^2$$

Jet vertex: LL versus NLL and k_T jet algorithm

NLL jet vertex and k_T algorithm

$\mathbf{k}, \mathbf{k}' =$ Euclidian two dimensional vectors

$$\mathcal{S}_J^{(3,\mathrm{k_T})}(\mathbf{k}', \mathbf{k}-\mathbf{k}', xz; x) =$$

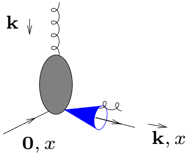

$$\mathcal{S}_J^{(2)}(\mathbf{k}, x)\, \Theta\left(R_{k_t}^2 - [\Delta y^2 + \Delta\phi^2]\right)$$

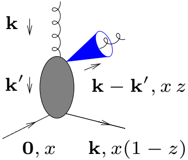

$$+\ \mathcal{S}_J^{(2)}(\mathbf{k}-\mathbf{k}', xz)\, \Theta\left([\Delta y^2 + \Delta\phi^2] - R_{k_t}^2\right)$$

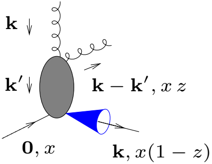

$$+\ \mathcal{S}_J^{(2)}(\mathbf{k}', x(1-z))\, \Theta\left([\Delta y^2 + \Delta\phi^2] - R_{k_t}^2\right),$$

Jet vertex: k_T and anti-k_T jet algorithms

anti-k_T algorithm (Cacciari, Salam, Soyez)

$$d_{ij} = \min\left(\frac{1}{p_i^2}, \frac{1}{p_j^2}\right)\frac{(y_i - y_j)^2 + (\phi_i - \phi_j)^2}{R_{k_t}^2}$$

$$d_{iB} = \frac{1}{p_i^2}$$

R_{k_t} = size parameter of the jet

- identify the smallest d_{ij}, d_{iB}
- if it is a d_{ij} combine i and j
- if it is a d_{iB}, i is considered as a jet
- this is done until all the particles are clustered into jets

main difference of k_T versus anti-k_T algorithms:

anti-k_T algorithm makes more circular profile in the (y, ϕ) plane

At NLO, same condition as for the k_T algorithm

Mueller-Navelet jets at NLL and finiteness

Using an IR safe jet algorithm, Mueller-Navelet jets at NLL are finite

- UV sector:
  - the NLL impact factor contains UV divergencies $1/\epsilon$
  - they are absorbed by the renormalization of the coupling: $\alpha_S \longrightarrow \alpha_S(\mu_R)$
- IR sector:
  - PDF have IR collinear singularities: pole $1/\epsilon$ at LO
  - these collinear singularities can be compensated by collinear singularities of the two jets vertices and the real part of the BFKL kernel
  - the remaining collinear singularities compensate exactly among themselves
  - soft singularities of the real and virtual BFKL kernel, and of the jets vertices compensates among themselves

This was shown for both quark and gluon initiated vertices (Bartels, Colferai, Vacca)

Master formulas

k_T-factorized differential cross section

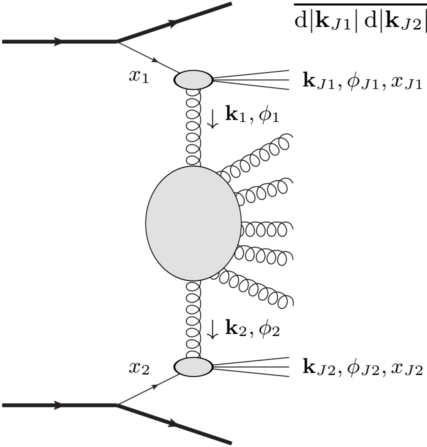

$$\frac{d\sigma}{d|\mathbf{k}_{J1}|\, d|\mathbf{k}_{J2}|\, dy_{J1}\, dy_{J2}} = \int d\phi_{J1}\, d\phi_{J2} \int d^2\mathbf{k}_1\, d^2\mathbf{k}_2$$

$$\times\, \Phi(\mathbf{k}_{J1}, x_{J1}, -\mathbf{k}_1)$$

$$\times\, G(\mathbf{k}_1, \mathbf{k}_2, \hat{s})$$

$$\times\, \Phi(\mathbf{k}_{J2}, x_{J2}, \mathbf{k}_2)$$

with $\Phi(\mathbf{k}_{J2}, x_{J2}, \mathbf{k}_2) = \int dx_2\, f(x_2) V(\mathbf{k}_2, x_2)$ $\qquad f \equiv$ PDF $\qquad x_J = \frac{|\mathbf{k}_J|}{\sqrt{s}} e^{y_J}$

Master formulas

It is useful to define the coefficients $\mathcal{C}_n$ as

$$\begin{aligned}\mathcal{C}_n \quad &\equiv \quad \int \mathrm{d}\phi_{J1}\,\mathrm{d}\phi_{J2}\,\cos\left(n(\phi_{J1}-\phi_{J2}-\pi)\right)\\ &\times \int \mathrm{d}^2\mathbf{k}_1\,\mathrm{d}^2\mathbf{k}_2\,\Phi(\mathbf{k}_{J1},x_{J1},-\mathbf{k}_1)\,G(\mathbf{k}_1,\mathbf{k}_2,\hat{s})\,\Phi(\mathbf{k}_{J2},x_{J2},\mathbf{k}_2)\end{aligned}$$

- $n = 0 \implies$ differential cross-section

$$\mathcal{C}_0 = \frac{\mathrm{d}\sigma}{\mathrm{d}|\mathbf{k}_{J1}|\,\mathrm{d}|\mathbf{k}_{J2}|\,\mathrm{d}y_{J1}\,\mathrm{d}y_{J2}}$$

- $n > 0 \implies$ azimuthal decorrelation

$$\frac{\mathcal{C}_n}{\mathcal{C}_0} = \langle\cos\left(n(\phi_{J,1}-\phi_{J,2}-\pi)\right)\rangle \equiv \langle\cos(n\varphi)\rangle$$

- sum over $n \implies$ azimuthal distribution

$$\frac{1}{\sigma}\frac{d\sigma}{d\varphi} = \frac{1}{2\pi}\left\{1 + 2\sum_{n=1}^{\infty}\cos(n\varphi)\,\langle\cos(n\varphi)\rangle\right\}$$

Master formulas in conformal variables

Rely on LL BFKL eigenfunctions

- LL BFKL eigenfunctions: $E_{n,\nu}(\mathbf{k}_1) = \frac{1}{\pi\sqrt{2}} \left(\mathbf{k}_1^2\right)^{i\nu-\frac{1}{2}} e^{in\phi_1}$
- decompose Φ on this basis
- use the known LL eigenvalue of the BFKL equation on this basis:

$$\omega(n,\nu) = \bar{\alpha}_s \chi_0 \left(|n|, \tfrac{1}{2} + i\nu\right)$$

with $\chi_0(n,\gamma) = 2\Psi(1) - \Psi\left(\gamma + \frac{n}{2}\right) - \Psi\left(1 - \gamma + \frac{n}{2}\right)$

$$(\Psi(x) = \Gamma'(x)/\Gamma(x),\ \bar{\alpha}_s = N_c \alpha_s/\pi)$$

- $\Longrightarrow$ master formula:

$$\mathcal{C}_m = (4 - 3\,\delta_{m,0}) \int \mathrm{d}\nu\, C_{m,\nu}(|\mathbf{k}_{J1}|, x_{J,1})\, C^*_{m,\nu}(|\mathbf{k}_{J2}|, x_{J,2}) \left(\frac{\hat{s}}{s_0}\right)^{\omega(m,\nu)}$$

with

$$C_{m,\nu}(|\mathbf{k}_J|, x_J) = \int \mathrm{d}\phi_J\, \mathrm{d}^2\mathbf{k}\, \mathrm{d}x\, f(x) V(\mathbf{k}, x) E_{m,\nu}(\mathbf{k}) \cos(m\phi_J)$$

- at NLL, same master formula: just change $\omega(m,\nu)$ and V

BFKL Green's function at NLL

NLL Green's function: rely on LL BFKL eigenfunctions

- NLL BFKLkernel is not conformal invariant
- LL $E_{n,\nu}$ are not anymore eigenfunction
- this can be overcome by considering the eigenvalue as an operator with a part containing $\frac{\partial}{\partial\nu}$
- it acts on the impact factor

$$\omega(n,\nu) = \bar{\alpha}_s \chi_0\left(|n|, \frac{1}{2}+i\nu\right) + \bar{\alpha}_s^2 \left[\chi_1\left(|n|, \frac{1}{2}+i\nu\right)\right.$$
$$\left. -\frac{\pi b_0}{2N_c}\chi_0\left(|n|, \frac{1}{2}+i\nu\right) \underbrace{\left\{-2\ln\mu_R^2 - i\frac{\partial}{\partial\nu}\ln\frac{C_{n,\nu}(|\mathbf{k}_{J1}|, x_{J,1})}{C_{n,\nu}(|\mathbf{k}_{J2}|, x_{J,2})}\right\}}_{2\ln\frac{|\mathbf{k}_{J1}|\cdot|\mathbf{k}_{J2}|}{\mu_R^2}}\right],$$

LL substraction and s_0 dependence

- one sums up $\sum(\alpha_s \ln \hat{s}/s_0)^n + \alpha_s \sum(\alpha_s \ln \hat{s}/s_0)^n \quad (\hat{s} = x_1\, x_2\, s)$
- at LL s_0 is arbitrary
- natural choice: $s_0 = \sqrt{s_{0,1}\, s_{0,2}} \quad s_{0,i}$ for each of the scattering objects
  - possible choice: $s_{0,i} = (|\mathbf{k}_J| + |\mathbf{k}_J - \mathbf{k}|)^2$ (Bartels, Colferai, Vacca)
    - but depend on $\mathbf{k}$, which is integrated over
    - $\hat{s}$ is not an external scale ($x_{1,2}$ are integrated over)
  - we prefer

$$\left.\begin{aligned} s_{0,1} &= (|\mathbf{k}_{J1}| + |\mathbf{k}_{J1} - \mathbf{k}_1|)^2 \;\to\; s'_{0,1} = \frac{x_1^2}{x_{J,1}^2}\mathbf{k}_{J1}^2 \\ s_{0,2} &= (|\mathbf{k}_{J2}| + |\mathbf{k}_{J2} - \mathbf{k}_2|)^2 \;\to\; s'_{0,2} = \frac{x_2^2}{x_{J,2}^2}\mathbf{k}_{J2}^2 \end{aligned}\right\} \quad \frac{\hat{s}}{s_0} \;\to\; \frac{\hat{s}}{s'_0} = \frac{x_{J,1}\, x_{J_2}\, s}{|\mathbf{k}_{J1}|\,|\mathbf{k}_{J2}|} = e^{y_{J,1}-y_{J,2}} \equiv e^Y$$

- $s_0 \to s'_0$ affects
  - the BFKL NLL Green function
  - the impact factors:

$$\Phi_{\rm NLL}(\mathbf{k}_i; s'_{0,i}) = \Phi_{\rm NLL}(\mathbf{k}_i; s_{0,i}) + \int \mathrm{d}^2\mathbf{k}'\, \Phi_{\rm LL}(\mathbf{k}'_i)\, \mathcal{K}_{\rm LL}(\mathbf{k}'_i, \mathbf{k}_i)\, \frac{1}{2} \ln \frac{s'_{0,i}}{s_{0,i}} \quad (1) \qquad (1)$$

- numerical stabilities (non azimuthal averaging of LL substraction) improved with the choice $s_{0,i} = (\mathbf{k}_i - 2\mathbf{k}_{Ji})^2$
  (then replaced by $s'_{0,i}$ after numerical integration)
- (1) can be used to test $s_0 \to \lambda\, s_0$ dependence

Collinear improvement at NLL

Collinear improved Green's function at NLL

- one may improve the NLL BFKL kernel for $n = 0$ by imposing its compatibility with DGLAP in the collinear limit
  Salam; Ciafaloni, Colferai
- usual (anti)collinear poles in $\gamma = 1/2 + i\nu$ (resp. $1-\gamma$) are shifted by $\omega/2$
- one practical implementation:
  - the new kernel $\bar{\alpha}_s \chi^{(1)}(\gamma, \omega)$ with shifted poles replaces

    $$\bar{\alpha}_s \chi_0(\gamma, 0) + \bar{\alpha}_s^2 \chi_1(\gamma, 0)$$

  - $\omega(0, \nu)$ is obtained by solving the implicit equation

    $$\omega(0, \nu) = \bar{\alpha}_s \chi^{(1)}(\gamma, \omega(0, \nu))$$

    for $\omega(n, \nu)$ numerically.
- there is no need for any jet vertex improvement because of the absence of γ and $1-\gamma$ poles (numerical proof using Cauchy theorem "backward")
- this can be extended for all n

Results

Results for a symmetric configuration

In the following we show results for

- $\sqrt{s} = 7$ TeV
- $35\,\mathrm{GeV} < |\mathbf{k}_{J1}|\,,|\mathbf{k}_{J2}| < 60\,\mathrm{GeV}$
- $0 < |y_1|\,,|y_2| < 4.7$

These cuts allow us to compare our predictions with the first experimental data on azimuthal correlations of Mueller-Navelet jets at the LHC obtained by CMS collaboration

note: unlike experiments we have to set an upper cut on $|\mathbf{k}_{J1}|$ and $|\mathbf{k}_{J2}|$. We have checked that our results do not depend on this cut significantly.

Results: symmetric configuration $(|\mathbf{k}_{J,1\ \mathrm{min}}| = |\mathbf{k}_{J,2\ \mathrm{min}}| = 35\,\mathrm{GeV})$ $\sqrt{s} = 7$ TeV

Azimuthal distribution

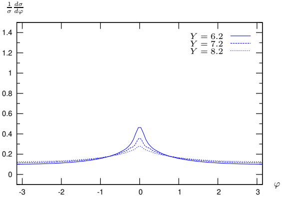

pure LL

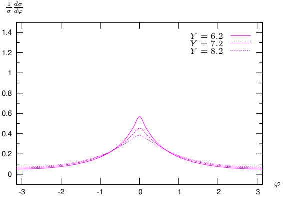

LL vertices + NLL Green's fun.

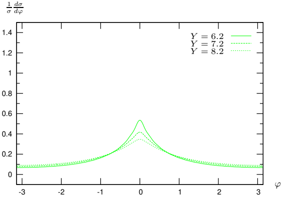

LL vert. + NLL resum. Green's fun.

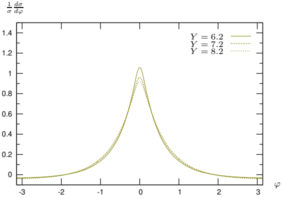

NLL vert. + NLL Green's fun.

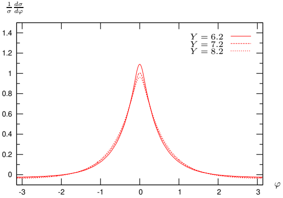

NLL vert. + NLL resum. Green's fun.

$$35\,\mathrm{GeV} < |\mathbf{k}_{J1}| < 60\,\mathrm{GeV}$$
$$35\,\mathrm{GeV} < |\mathbf{k}_{J2}| < 60\,\mathrm{GeV}$$

$$0 < Y_1 < 4.7$$
$$0 < Y_2 < 4.7$$

Full NLL treatment predicts :

- Less decorrelation for the same Y
- Slower decorrelation with increasing Y

Results: symmetric configuration $(|\mathbf{k}_{J,1\,\mathrm{min}}| = |\mathbf{k}_{J,2\,\mathrm{min}}| = 35\,\mathrm{GeV})$ $\sqrt{s} = 7$ TeV

Azimuthal distribution: stability with respect to s_0 and $\mu_R = \mu_F$

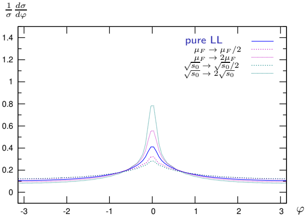

pure LL

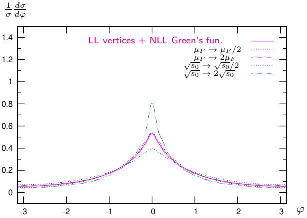

LL vertices + NLL Green's fun.

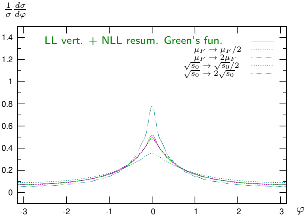

LL vert. + NLL resum. Green's fun.

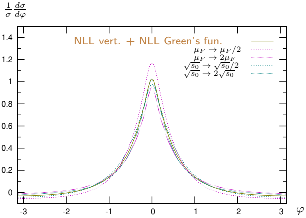

NLL vert. + NLL Green's fun.

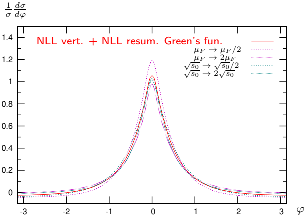

NLL vert. + NLL resum. Green's fun.

$35\,\mathrm{GeV} < |\mathbf{k}_{J1}| < 60\,\mathrm{GeV}$
$35\,\mathrm{GeV} < |\mathbf{k}_{J2}| < 60\,\mathrm{GeV}$

$0 < Y_1 < 4.7$
$0 < Y_2 < 4.7$
integrating on the bin:
$6 < Y = Y_1 + Y_2 < 9.4$

The predicted φ distribution within full NLL treatment is stable

Results: azimuthal correlations

Azimuthal correlation $\langle \cos \varphi \rangle$

$$\frac{\mathcal{C}_1}{\mathcal{C}_0} = \langle \cos \varphi \rangle \equiv \langle \cos(\phi_{J1} - \phi_{J2} - \pi) \rangle$$

recall: $\varphi = 0 \Leftrightarrow$ back-to-back

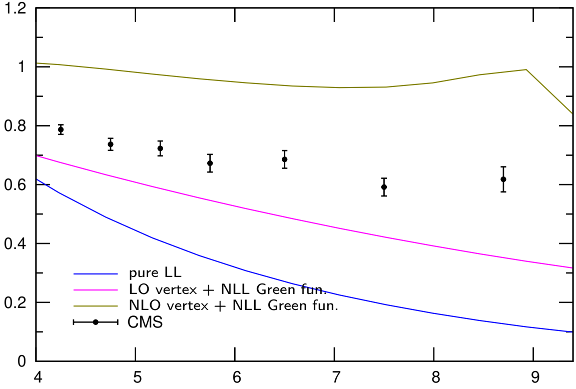

$Y \equiv |y_1 - y_2|$

$35 \text{ GeV} < |\mathbf{k}_{J1}| < 60 \text{ GeV}$

$35 \text{ GeV} < |\mathbf{k}_{J2}| < 60 \text{ GeV}$

$0 < |y_1| < 4.7$

$0 < |y_2| < 4.7$

The NLO corrections to the jet vertex lead to a large increase of the correlation

Note: LO vertex + NLL Green done by F. Schwennsen, A. Sabio-Vera; C. Marquet, C. Royon

Results: azimuthal correlations

Azimuthal correlation $\langle \cos \varphi \rangle$

$\langle \cos \varphi \rangle \equiv \langle \cos(\phi_{J1} - \phi_{J2} - \pi) \rangle$

recall: $\varphi = 0 \Leftrightarrow$ back-to-back

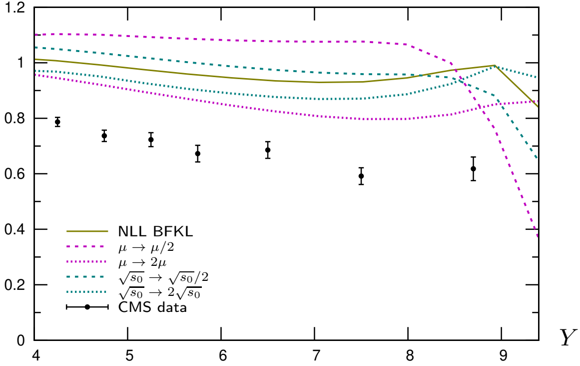

$35\,\mathrm{GeV} < |\mathbf{k}_{J1}| < 60\,\mathrm{GeV}$
$35\,\mathrm{GeV} < |\mathbf{k}_{J2}| < 60\,\mathrm{GeV}$

$0 < |y_1| < 4.7$
$0 < |y_2| < 4.7$

- NLL BFKL predicts a too small decorrelation
- The NLL BFKL calculation is still rather dependent on the scales, especially the renormalization / factorization scale

Results: azimuthal correlations

Azimuthal correlation $\langle\cos 2\varphi\rangle$

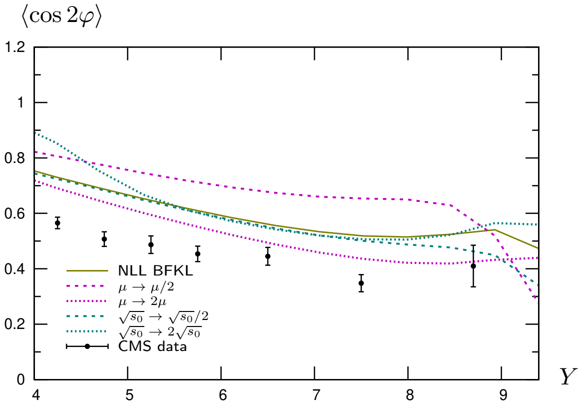

recall: $\varphi = 0 \Leftrightarrow$ back-to-back

$35\ \mathrm{GeV} < |\mathbf{k}_{J1}| < 60\ \mathrm{GeV}$

$35\ \mathrm{GeV} < |\mathbf{k}_{J2}| < 60\ \mathrm{GeV}$

$0 < |y_1| < 4.7$

$0 < |y_2| < 4.7$

- The agreement with data is a little better for $\langle\cos 2\varphi\rangle$ but still not very good
- This observable is also very sensitive to the scales

Results: azimuthal correlations

Azimuthal correlation $\langle \cos 2\varphi \rangle / \langle \cos \varphi \rangle$

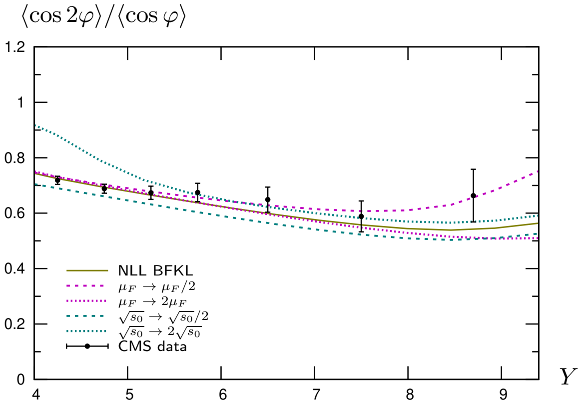

recall: $\varphi = 0 \Leftrightarrow$ back-to-back

$35\,\text{GeV} < |\mathbf{k}_{J1}| < 60\,\text{GeV}$
$35\,\text{GeV} < |\mathbf{k}_{J2}| < 60\,\text{GeV}$

$0 < |y_1| < 4.7$
$0 < |y_2| < 4.7$

- This observable is more stable with respect to the scales than the previous ones
- The agreement with data is good across the whole Y range

Results: azimuthal correlations

Azimuthal correlation $\langle \cos 2\varphi \rangle / \langle \cos \varphi \rangle$

recall: $\varphi = 0 \Leftrightarrow$ back-to-back

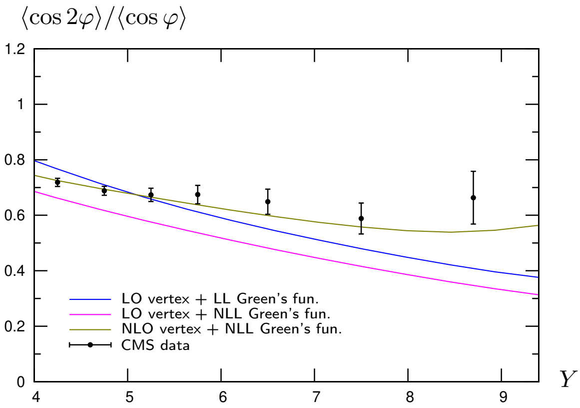

$35\,\text{GeV} < |\mathbf{k}_{J1}| < 60\,\text{GeV}$
$35\,\text{GeV} < |\mathbf{k}_{J2}| < 60\,\text{GeV}$

$0 < |y_1| < 4.7$
$0 < |y_2| < 4.7$

It is necessary to include the NLO corrections to the jet vertex to reproduce the behavior of the data at large Y

Results: azimuthal distribution

Azimuthal distribution (integrated over $6 < Y < 9.4$)

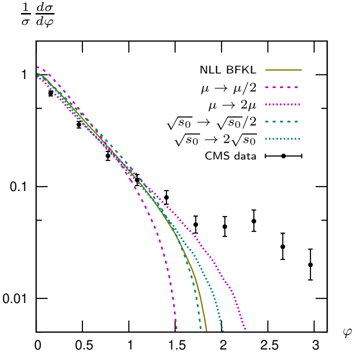

recall: $\varphi = 0 \Leftrightarrow$ back-to-back

$$\frac{1}{\sigma}\frac{d\sigma}{d\varphi} = \frac{1}{2\pi}\left\{1 + 2\sum_{n=1}^{\infty}\cos(n\varphi)\,\langle\cos(n\varphi)\rangle\right\}.$$

- Our calculation predicts a too large value of $\frac{1}{\sigma}\frac{d\sigma}{d\varphi}$ for $\varphi \lesssim \frac{\pi}{2}$ and a too small value for $\varphi \gtrsim \frac{\pi}{2}$
- It is not possible to describe the data even when varying the scales by a factor of 2

Results: limitations

- The agreement of our calculation with the data for $\langle \cos 2\varphi \rangle / \langle \cos \varphi \rangle$ is good and quite stable with respect to the scales
- The agreement for $\langle \cos n\varphi \rangle$ and $\frac{1}{\sigma} \frac{d\sigma}{d\varphi}$ is not very good and very sensitive to the choice of the renormalization scale μ_R
- An all-order calculation would be independent of the choice of μ_R. This feature is lost if we truncate the perturbative series
  $\Rightarrow$ How to choose the renormalization scale?
  'Natural scale': sometimes the typical momenta in a loop diagram are different from the natural scale of the process

We decided to use the Brodsky-Lepage-Mackenzie (BLM) procedure to fix the renormalization scale

The BLM renormalization scale fixing procedure

- The Brodsky-Lepage-Mackenzie (BLM) procedure resums the self-energy corrections to the gluon propagator at one loop into the running coupling.
- Applications to BFKL:
  LL: S. J. Brodsky, F. Hautmann, D. E. Soper
  NLL:
  S. J. Brodsky, V. S. Fadin, V. T. Kim, L. N. Lipatov, G. B. Pivovarov
  M. Angioni, G. Chachamis, J. D. Madrigal, A. Sabio Vera
  M. Hentschinski, A. Sabio Vera, C. Salas
  F. Caporale, D. Yu. Ivanov, B. Murdaca, A. Papa
- Brodsky, Fadin, Kim, Lipatov and Pivovarov suggested that:
  - one should first go to a physical renormalization scheme like MOM
  - then apply the 'traditional' BLM procedure, i.e. identify the β_0 dependent part and choose μ_R such that it vanishes
- We followed this prescription for the full amplitude at NLL.

Results with BLM

Azimuthal correlation $\langle \cos\varphi \rangle$

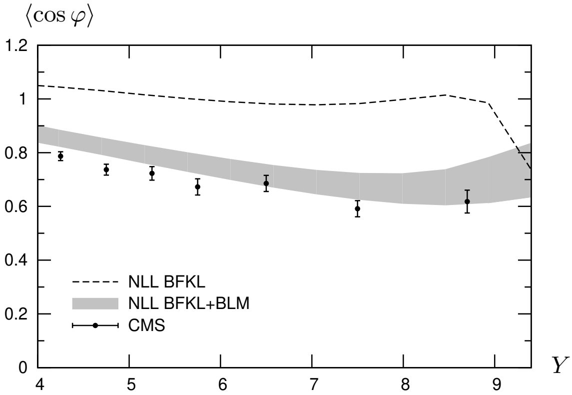

$35\,\text{GeV} < |\mathbf{k}_{J1}| < 60\,\text{GeV}$
$35\,\text{GeV} < |\mathbf{k}_{J2}| < 60\,\text{GeV}$

$0 < |y_1| < 4.7$
$0 < |y_2| < 4.7$

anti-k_T jet algorithm
$R = 0.5$

Using the BLM scale setting, the agreement with data becomes much better

Results with BLM

Azimuthal correlation $\langle \cos 2\varphi \rangle$

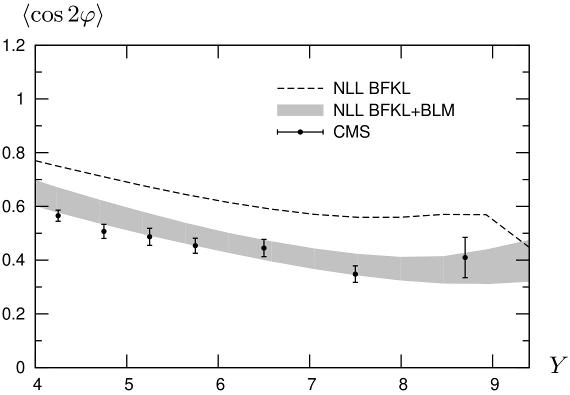

$35\ \mathrm{GeV} < |\mathbf{k}_{J1}| < 60\ \mathrm{GeV}$
$35\ \mathrm{GeV} < |\mathbf{k}_{J2}| < 60\ \mathrm{GeV}$

$0 < |y_1| < 4.7$
$0 < |y_2| < 4.7$

anti-k_T jet algorithm
$R = 0.5$

Using the BLM scale setting, the agreement with data becomes much better.

Results with BLM

Azimuthal correlation $\langle \cos 2\varphi \rangle / \langle \cos \varphi \rangle$

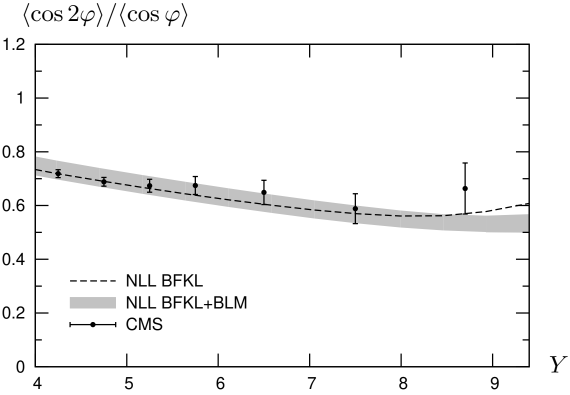

$35 \text{ GeV} < |\mathbf{k}_{J1}| < 60 \text{ GeV}$
$35 \text{ GeV} < |\mathbf{k}_{J2}| < 60 \text{ GeV}$

$0 < |y_1| < 4.7$
$0 < |y_2| < 4.7$

anti-k_T jet algorithm
$R = 0.5$

Because it is much less dependent on the scales, the observable $\langle \cos 2\varphi \rangle / \langle \cos \varphi \rangle$ is almost not affected by the BLM procedure and is still in good agreement with the data.

Results with BLM

Azimuthal distribution (integrated over $6 < Y < 9.4$)

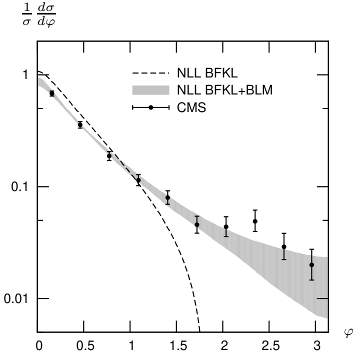

With the BLM scale setting the azimuthal distribution is in very good agreement with the data across the full φ range.

CMS measurement versus theory within various alternative descriptions

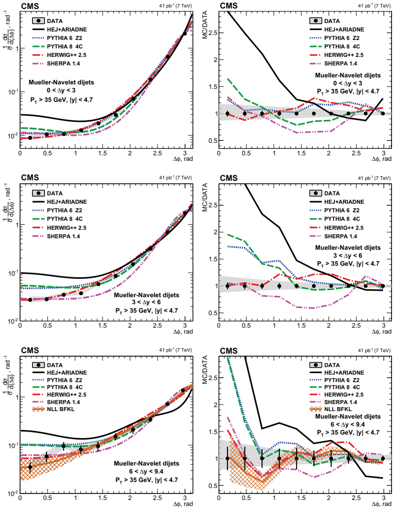

Figure 1: Left: Distributions of the azimuthal-angle difference, $\Delta\phi$, between MN jets in the rapidity intervals $\Delta y < 3.0$ (top row), $3.0 < \Delta y < 6.0$ (centre row), and $6.0 < \Delta y < 9.4$ (bottom row). Right: Ratios of predictions to the data in the corresponding rapidity intervals. The data (points) are plotted with experimental statistical (systematic) uncertainties indicated by the error bars (the shaded band), and compared to predictions from the LL DGLAP-based MC generators PYTHIA 6, PYTHIA 8, HERWIG++, and SHERPA, and to the LL BFKL-motivated MC generator HEJ with hadronisation performed with ARIADNE (solid line).

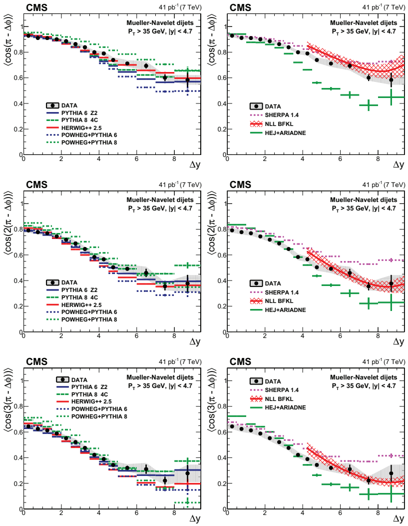

Figure 2: Left: Average $\langle\cos(n(\pi - \Delta\phi))\rangle(n = 1, 2, 3)$ as a function of Δy compared to LL DGLAP MC generators. In addition, the predictions of the NLO generator POWHEG interfaced with the LL DGLAP generators PYTHIA 6 and PYTHIA 8 are shown. Right: Comparison of the data to the MC generator SHERPA with parton matrix elements matched to a LL DGLAP parton shower, to the LL BFKL inspired generator HEJ with hadronisation by ARIADNE, and to analytical NLL BFKL calculations at the parton level ($4.0 < \Delta y < 9.4$).

Comparison with fixed-order

Using the BLM scale setting:

- The agreement $\langle \cos n\varphi \rangle$ with the data becomes much better
- The agreement for $\langle \cos 2\varphi \rangle / \langle \cos \varphi \rangle$ is still good and unchanged as this observable is weakly dependent on μ_R
- The azimuthal distribution is in much better agreement with the data

But the configuration chosen by CMS with $|\mathbf{k}_{J1}|_{\min} = |\mathbf{k}_{J2}|_{\min}$ does not allow us to compare with a fixed-order $\mathcal{O}(\alpha_s^3)$ treatment (i.e. without resummation)

- These calculations are unstable when $|\mathbf{k}_{J1}|_{\min} = |\mathbf{k}_{J2}|_{\min}$ because the cancellation of some IR divergencies is difficult to obtain numerically
- Resummation effects à la Sudakov are important in the limit $\mathbf{k}_{J1} \simeq -\mathbf{k}_{J2}$ and require a special treatment.
    - This resummation has been obtained at LL
      A. H. Mueller, L. Szymanowski, S. W., B.-W. Xiao, F. Yuan
    - The evaluation of the magnitude of this effect remains to be done
    - Beyond LL, it is presumably very tricky ...
- This resummation is not available in fixed-order treatments

Motivation for asymmetric configurations

- Initial (and final) state radiation (unseen) produces divergencies if one touches the collinear singularity $\mathbf{q}^2 \to 0$

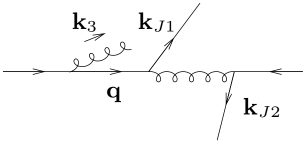

- they are compensated by virtual corrections
- this compensation is in practice difficult to implement, or *even incomplete*, when for some reason this additional emission is in a "corner" of the phase space (dip in the differential cross-section)
- this is the case when $\mathbf{k}_{J1} + \mathbf{k}_{J2} \to 0$
- this calls for a resummation of large remaing logs $\Rightarrow$ Sudakov resummation

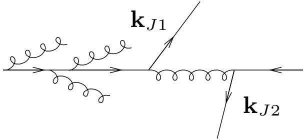

Motivation for asymmetric configurations

- since these resummation have never been investigated in this context, one should better avoid that region
- note that for BFKL, due to additional emission between the two jets, one may expect a less severe problem (at least a smearing in the dip region $|\mathbf{k}_{J1}| \sim |\mathbf{k}_{J2}|$)

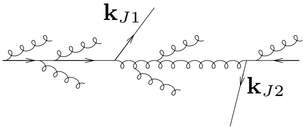

- this may however not mean that the region $|\mathbf{k}_{J1}| \sim |\mathbf{k}_{J2}|$ is perfectly trustable even in a BFKL type of treatment:
  in the limit $q_\perp^2 \equiv (\mathbf{k}_{J1} + \mathbf{k}_{J2})^2 \ll \tilde{P}_\perp^2 \equiv |\mathbf{k}_{J1}||\mathbf{k}_{J2}|$, at one-loop,

$$S_{qq\to qq} = -\frac{\alpha_s C_F}{2\pi} \ln^2 \frac{\tilde{P}_\perp^2 R_\perp^2}{c_0^2} \qquad (c_0 = 2e^{-\gamma_E})$$

  impact parameter $R_\perp \xleftrightarrow{\text{Fourier}}$ momentum imbalance $q_\perp$
  $R_\perp \sim 1/q_\perp \Rightarrow$ suppression of this back-to-back configuration
  (on top of BFKL large Y effects)
- we thus think that a measurement in a region where both NLO fixed order and NLL BFKL are under control would be safer!

Factorization of Sudakov double logs and of BFKL dynamics

One-loop analysis and factorization of the differential cross section

- Collinear and soft gluon radiations $\Rightarrow$ incoming partons gets a $q_\perp$
- These radiations are controlled by the Sudakov formalism and can be derived formally by the Collins-Soper-Sterman resummation
- Each of the incoming partons with a $q_\perp$ scatter off each other by exchanging a $t-$channel gluon, dominated by the BFKL dynamics

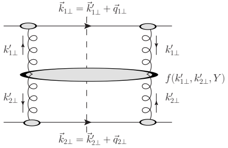

$$\frac{d\sigma}{dy_1 dy_2 d^2k_{1\perp} d^2k_{2\perp}} = \int d^2q_{1\perp} d^2q_{2\perp} \mathcal{F}_a(x_1, q_{1\perp}; \mu = k_{1\perp}) \mathcal{F}_b(x_2, q_{2\perp}; \mu = k_{2\perp}) \times \hat{\sigma}_{ab}(k_{1\perp}, k_{2\perp}; \mu) f_{BFKL}(\vec{k}_{1\perp} - \vec{q}_{1\perp}, \vec{k}_{2\perp} - \vec{q}_{2\perp}; Y)$$

- $\hat{\sigma}_{ab}$: partonic cross section
- $\mathcal{F}_{a,b}$: transverse momentum distributions (TMDs) with Sudakov resummation effects including initial and final state radiations:

$$\mathcal{F}_a(x, q_\perp; \mu_F = k_\perp) = x \int \frac{d^2R_\perp}{(2\pi)^2} e^{iq_\perp \cdot R_\perp} e^{-\mathcal{S}^a_{sud}(\mu_F = k_\perp, R_\perp)} C \otimes f_a(x, \mu_b)$$

  - $f_{q,g}(x, \mu_b)$: integrated q/g distribution functions at the scale $\mu_b = c_0/R_\perp$
  - $C \otimes f_{q,g}$: convolution integral for the parton distributions

$$C \otimes f_a(x, \mu) = \int \frac{dx'}{x'} \sum_i C_{a/i}(x/x') f_i(x', \mu)$$

Comparison with fixed-order

Results for an asymmetric configuration

In this section we choose the cuts as

- $35\,\mathrm{GeV} < |\mathbf{k}_{J1}|\,, |\mathbf{k}_{J2}| < 60\,\mathrm{GeV}$
- $50\,\mathrm{GeV} < \mathrm{Max}(|\mathbf{k}_{J1}|, |\mathbf{k}_{J2}|)$
- $0 < |y_1|\,, |y_2| < 4.7$

and we compare our results with the NLO fixed-order code Dijet (Aurenche, Basu, Fontannaz) in the same configuration

Comparison with fixed-order

Azimuthal correlation $\langle \cos \varphi \rangle$

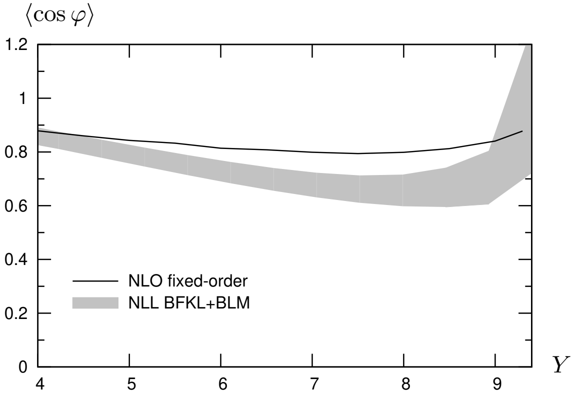

$35\,\mathrm{GeV} < |\mathbf{k}_{J1}| < 60\,\mathrm{GeV}$

$35\,\mathrm{GeV} < |\mathbf{k}_{J2}| < 60\,\mathrm{GeV}$

$50\,\mathrm{GeV} < \mathrm{Max}(|\mathbf{k}_{J1}|, |\mathbf{k}_{J2}|)$

$0 < |y_1| < 4.7$

$0 < |y_2| < 4.7$

The NLO fixed-order and NLL BFKL+BLM calculations are very close

Comparison with fixed-order

Azimuthal correlation $\langle \cos 2\varphi \rangle$

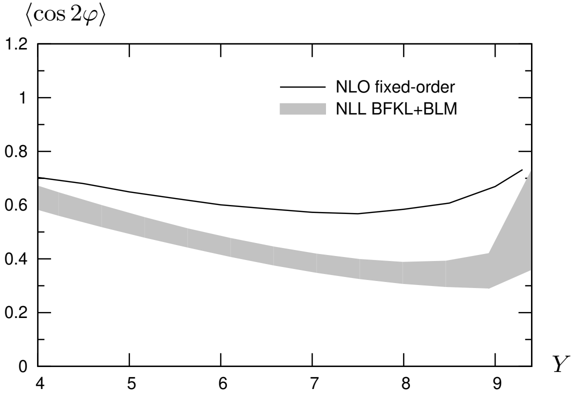

$$35 \text{ GeV} < |\mathbf{k}_{J1}| < 60 \text{ GeV}$$
$$35 \text{ GeV} < |\mathbf{k}_{J2}| < 60 \text{ GeV}$$
$$50 \text{ GeV} < \text{Max}(|\mathbf{k}_{J1}|, |\mathbf{k}_{J2}|)$$

$$0 < |y_1| < 4.7$$
$$0 < |y_2| < 4.7$$

The BLM procedure leads to a sizable difference between NLO fixed-order and NLL BFKL+BLM.

Comparison with fixed-order

Azimuthal correlation $\langle \cos 2\varphi \rangle / \langle \cos \varphi \rangle$

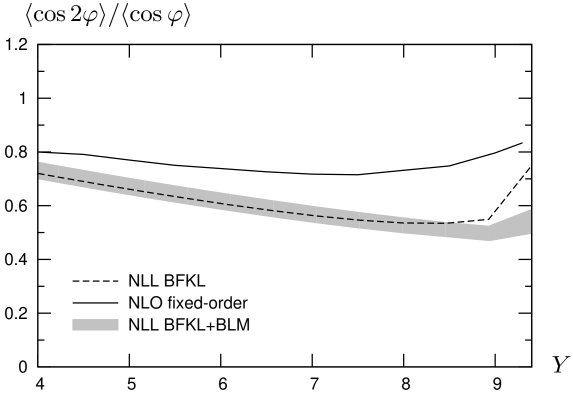

$35\,\mathrm{GeV} < |\mathbf{k}_{J1}| < 60\,\mathrm{GeV}$

$35\,\mathrm{GeV} < |\mathbf{k}_{J2}| < 60\,\mathrm{GeV}$

$50\,\mathrm{GeV} < \mathrm{Max}(|\mathbf{k}_{J1}|, |\mathbf{k}_{J2}|)$

$0 < |y_1| < 4.7$

$0 < |y_2| < 4.7$

Using BLM or not, there is a sizable difference between BFKL and fixed-order.

Comparison with fixed-order

Cross section: 13 TeV vs. 7 TeV

back to the original idea of Mueller and Navelet

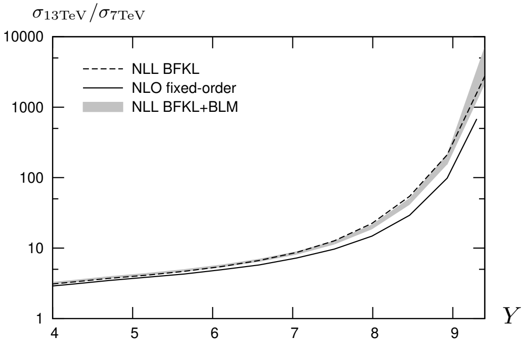

$35\,\text{GeV} < |\mathbf{k}_{J1}| < 60\,\text{GeV}$

$35\,\text{GeV} < |\mathbf{k}_{J2}| < 60\,\text{GeV}$

$50\,\text{GeV} < \text{Max}(|\mathbf{k}_{J1}|, |\mathbf{k}_{J2}|)$

$0 < |y_1| < 4.7$

$0 < |y_2| < 4.7$

- In a BFKL treatment, a strong rise of the cross section with increasing energy is expected.
- This rise is faster for LL BFKL than in a fixed-order treatment
- this remains true within a NLL BFKL treatment

Comparison with fixed-order

Cross section: 13 TeV vs. 7 TeV

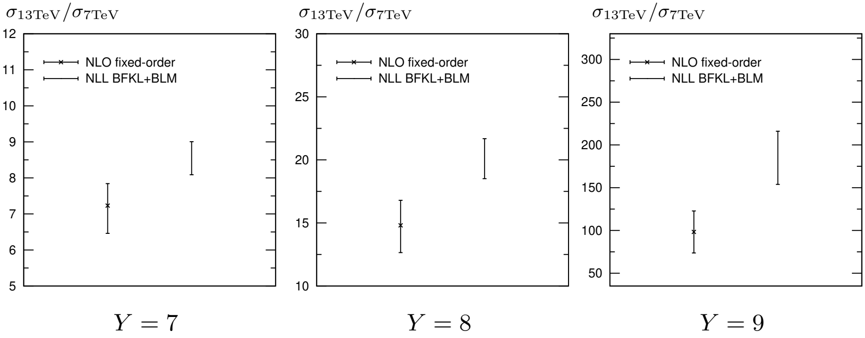

caveat: with scale + PDF uncertainties, the difference is less pronounced still:

- higher $s \Rightarrow$ at fixed Y, x inside PDFs reduce $\Rightarrow$ statistics increase
- thus, higher precision expected at 13 TeV than 7 TeV

Energy-momentum conservation

- It is necessary to have $\mathbf{k}_{J\mathrm{min}1} \neq \mathbf{k}_{J\mathrm{min}2}$ for comparison with fixed order calculations but this can be problematic for BFKL because of energy-momentum conservation
- There is no strict energy-momentum conservation in BFKL
- This was studied at LO by V. Del Duca and C. R. Schmidt. They introduced an effective rapidity Y_{eff} defined as

$$Y_{\mathrm{eff}} \equiv Y \frac{\sigma^{2\to 3}}{\sigma^{\mathrm{BFKL},\mathcal{O}(\alpha_s^3)}}$$

- When one replaces Y by Y_{eff} in the expression of σ^{BFKL} and truncates to $\mathcal{O}(\alpha_s^3)$, the exact $2 \to 3$ result is obtained

Energy-momentum conservation

We follow the idea of Del Duca and Schmidt, adding the NLO jet vertex contribution:

exact $2 \to 3$

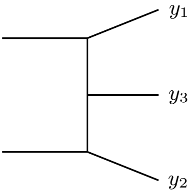

BFKL

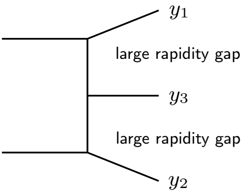

one emission from the Green's function + LO jet vertex

we have to take into account these additional $\mathcal{O}(\alpha_s^3)$ contributions:

+

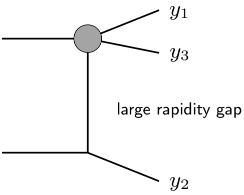

+

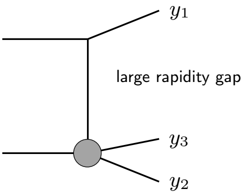

no emission from the Green's function + NLO jet vertex

Energy-momentum conservation

Variation of $Y_{\rm eff}/Y$ as a function of $\mathbf{k}_{J2}$ for fixed $\mathbf{k}_{J1} = 35$ GeV (with $\sqrt{s} = 7$ TeV, $Y = 8$):

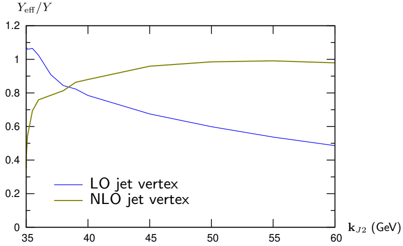

- With the LO jet vertex, $Y_{\rm eff}$ is much smaller than Y when $\mathbf{k}_{J1}$ and $\mathbf{k}_{J2}$ are significantly different
- This is the region important for comparison with fixed order calculations
- The improvement coming from the NLO jet vertex is very large in this region
- For $\mathbf{k}_{J1} = 35$ GeV and $\mathbf{k}_{J2} = 50$ GeV, typical of the values we used for comparison with fixed order, we get $\frac{Y_{\rm eff}}{Y} \simeq 0.98$ at NLO vs. ~ 0.6 at LO

Can Mueller-Navelet jets be a manifestation of multiparton interactions?

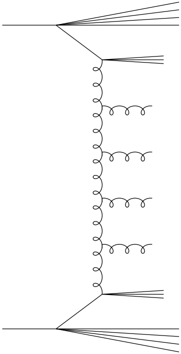

+

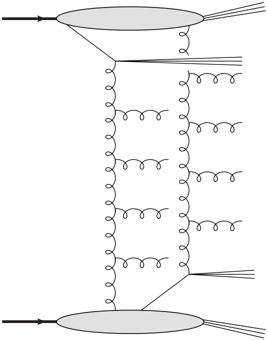

MN jets in the single partonic model

MN jets in MPI

here MPI = DPS (double parton scattering)

Can Mueller-Navelet jets be a manifestation of multiparton interactions?

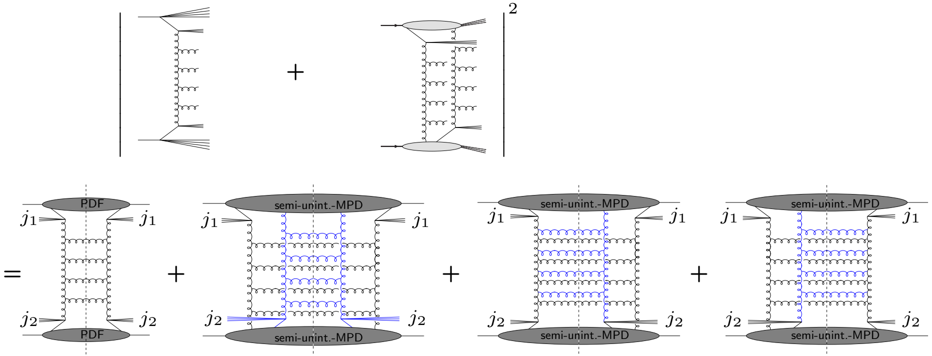

single $\mathbb{P}$ ladder	two $\mathbb{P}$ ladders	interferences
scaling: $s^{\alpha_{\mathbb{P}}}$	$(??)\ s^{2\alpha_{\mathbb{P}}}$	??

- The twist counting is not easy for MPI kinds of contributions at small x
- $k_{\perp 1,2}$ are not integrated $\Rightarrow$ MPI may be competitive, and enhanced by small-x resummation
- Interference terms are not governed by BJKP (this is not a fully interacting 3-reggeons system) (for BJKP, $\alpha_{\mathbb{P}} < 1 \Rightarrow$ suppressed)

A phenomenological test: the problem

- Simplification: we neglect any interference contribution between the two mecchanisms
- How to evaluate the DPS contribution?

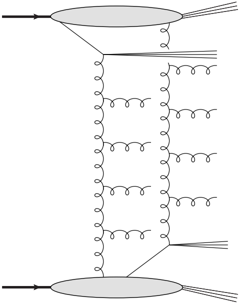

- This would require some kind of "hybrid" double parton distributions, with
  - one collinear parton
  - one off-shell parton (with some $k_\perp$)
- Almost nothing is known on such distributions

A phenomenological test: our ansatz

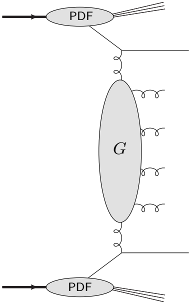

Mueller-Navelet jets production at LL accuracy

$\longrightarrow$

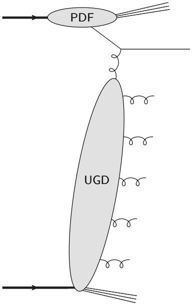

Inclusive forward jet production

Factorized ansatz for the DPS contribution:

$$\sigma_{\mathrm{DPS}} = \frac{\sigma_{\mathrm{fwd}} \; \sigma_{\mathrm{bwd}}}{\sigma_{\mathrm{eff}}}$$

Tevatron, LHC: $\sigma_{\mathrm{eff}} \simeq 15$ mb

To account for some discrepancy between various measurements, we take

$$\sigma_{\mathrm{eff}} \simeq 10 - 20 \text{ mb}$$

A phenomenological test: our ansatz

At LO for the jet vertex:

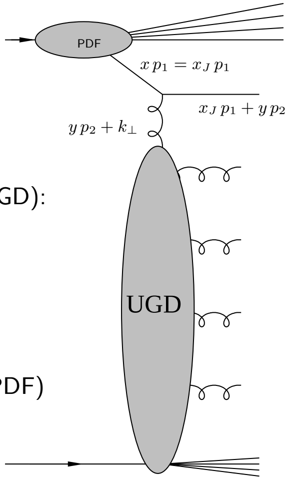

$\left(y = \frac{\mathbf{k}_J^2}{s x_J}\right.$: on-shell cond.)

unintegrated gluon distribution (UGD):

$$\mathcal{F}_g\left(\frac{\mathbf{k}_J^2}{s\,x_J}, |\mathbf{k}_J|\right)$$

normalized according to:

$\int \mathrm{d}\mathbf{k}^2 \mathcal{F}_g(x, |\mathbf{k}|) = x f_g(x)$ (usual PDF)

inclusive forward jet cross-section:

$$\frac{\mathrm{d}\sigma}{\mathrm{d}|\mathbf{k}_J|\mathrm{d}y_J} = K\,\frac{\alpha_s}{|\mathbf{k}_J|}\,x_J\,(C_F\,f_q(x_J) + C_A\,f_g(x_J))\,\mathcal{F}_g\left(\frac{\mathbf{k}_J^2}{s\,x_J}, |\mathbf{k}_J|\right)$$

A phenomenological test

- We use CMS data at $\sqrt{s} = 7$ TeV, $3.2 < |y_J| < 4.7$
- We use various parametrization for the UGD
- For each parametrization we determine the range of K compatible with the CMS measurement in the lowest transverse momentum bin

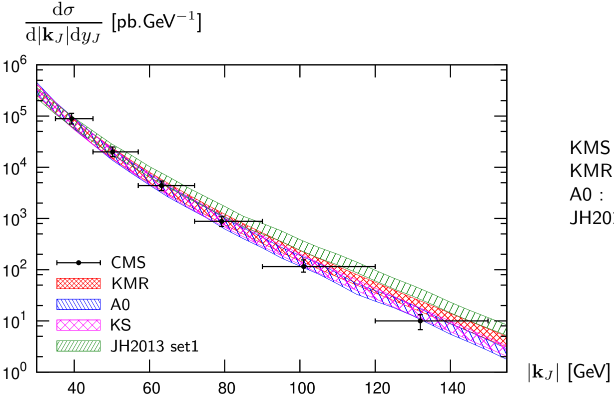

	K_{min}	K_{max}
KMS :	1.20	1.94
KMR :	1.05	1.69
A0 :	4.27	6.89
JH2013 :	2.44	3.94

$$\frac{d\sigma}{d|\mathbf{k}_J|dy_J} = K \frac{\alpha_s}{|\mathbf{k}_J|} x_J \left(C_F f_q(x_J) + C_A f_g(x_J)\right) \mathcal{F}_g\left(\frac{\mathbf{k}_J^2}{s\, x_J}, |\mathbf{k}_J|\right)$$

SPS vs DPS: Results

We focus on four choices of kinematical cuts:

- $\sqrt{s} = 7$ TeV, $|\mathbf{k}_{J1}| = |\mathbf{k}_{J2}| = 35$ GeV,
  (like in the CMS analysis for azimuthal correlations of MN jets)
- $\sqrt{s} = 14$ TeV, $|\mathbf{k}_{J1}| = |\mathbf{k}_{J2}| = 35$ GeV,
- $\sqrt{s} = 14$ TeV, $|\mathbf{k}_{J1}| = |\mathbf{k}_{J2}| = 20$ GeV,
- $\sqrt{s} = 14$ TeV, $|\mathbf{k}_{J1}| = |\mathbf{k}_{J2}| = 10$ GeV $\leftarrow$ highest DPS effect expected

parameters:

- $0 < y_{J,1} < 4.7$ and $-4.7 < y_{J,2} < 0$
- MSTW 2008 parametrization for PDFs
- In the case of the NLL NFKL calculation, anti-k_t jet algorithm with $R = 0.5$.

SPS vs DPS: cross-sections

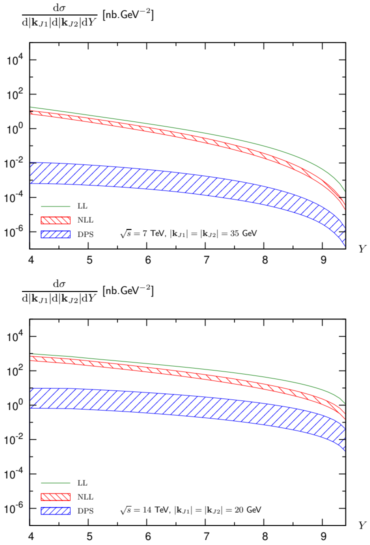

SPS vs DPS: cross-sections (ratios)

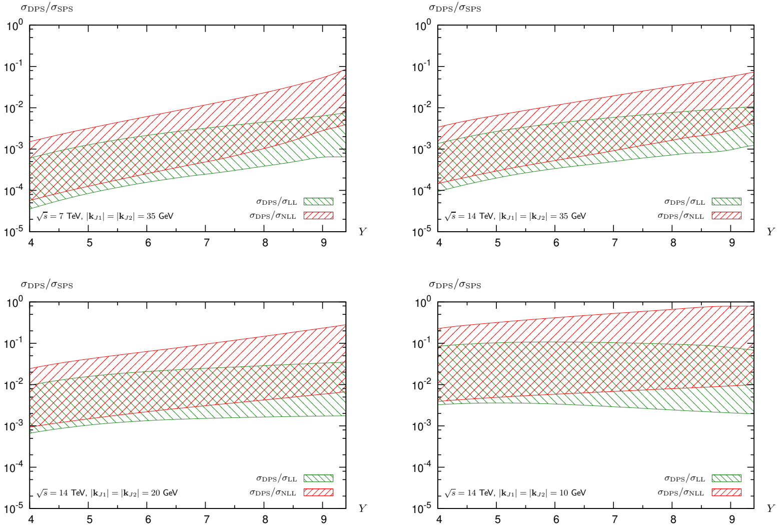

SPS vs DPS: Azimuthal correlations

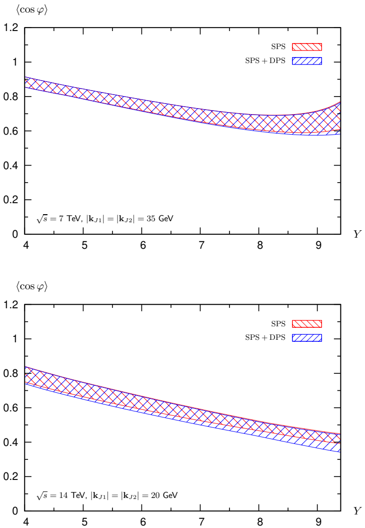

SPS vs DPS: Azimuthal distributions

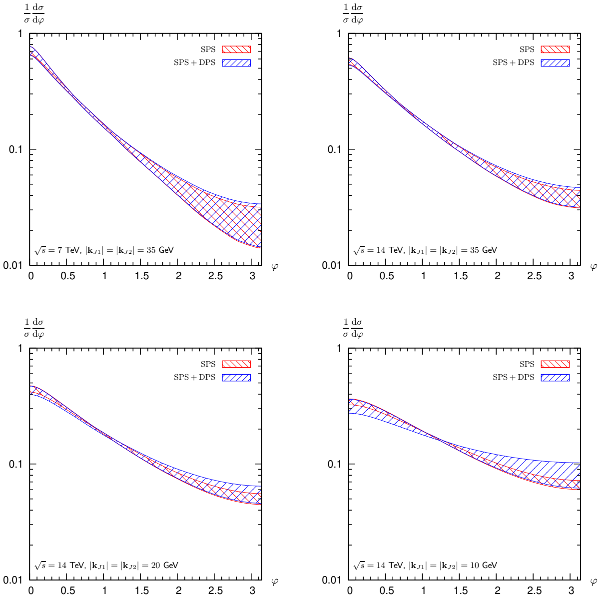

$$8 < Y < 9.4$$

Inclusive production of a forward J/ψ + a backward jet

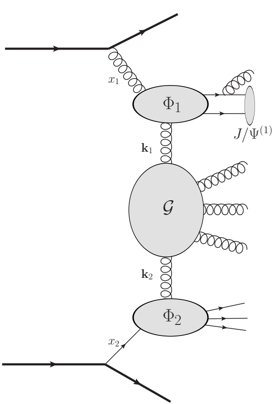

Color singlet mechanism

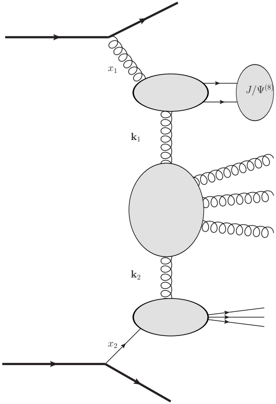

Color octet mechanism

- Hard scales: $\mathbf{k}_J$ and $M_{J/\psi}$
- 2 mechanisms:
  - naive color evaporation model
  - Non Relativistic QCD (NRQCD): singlet + color octet contributions
- Very promising at ATLAS and CMS

R. Boussarie, B. Ducloué, L. Szymanowski, S. W. **[See backup]**

Conclusions

- (di)Jets are among the best observables to access the QCD high energy dynamics
- Mueller-Navelet jets at full (vertex + Green's function) NLL BFKL accuracy, improved by using the BLM scale fixing procedure, gives a very good description of CMS data at 7 TeV for dijet azimuthal distribution
- To be fully conclusive with respect to fixed order descriptions, one should consider asymmetric configuration
- Sudakov resummation is expect to reduce the back-to-back configuration; it factorizes with BFKL dynamics at one loop
- $\langle \cos 2\varphi \rangle / \langle \cos \varphi \rangle$ is almost not affected by BLM and shows a clear difference between NLO fixed-order and NLL BFKL in an asymmetric configuration
- Energy-momentum conservation much improved with the NLO jet vertex
- A sizable difference is expected between NLLx and NLLQ descriptions of the ratio of cross-sections with different s
- For large Y and low $\mathbf{k}_J$ jets, the effect of DPS can become larger than the uncertainty on the NLL BFKL calculation.
- Exclusive diffractive production of dijets
  (in UPC (LHC) or in photo/electroproduction (EIC, LHeC))
  is a perfect way to perform precision physics (NLO) of gluonic saturation and to get access to the Wigner gluon distribution

Backup

Inclusive forward J/Ψ and backward jet production at the LHC

Why J/Ψ?

- Numerous J/ψ mesons are produced at LHC
- J/ψ is "easy" to reconstruct experimentaly through its decay to $\mu^+\mu^-$ pairs
- The mechanism for the production of J/ψ mesons is still to be completely understood (see discussion later), although it was observed more than 40 years ago E598 collab 1974; SLAC-SP collab 1974
- Any improvement of the understanding of these mechanisms is important in view of QGP studies since J/Ψ suppression (melting) is one of the best probe. Cold nuclear effects are numerous and known to make life more complicate
- The vast majority of J/ψ theoretical predictions are done in the collinear factorization framework : would k_t factorization give something different?
- We performed an MN-like analysis, considering a process with a rapidity difference which is large enough to use BFKL dynamics but small enough to be able to detect J/ψ mesons at LHC (ATLAS, CMS).

Master formula

$k_\perp$-factorization description of the process

$\hat{s} = x\,x'\,s$

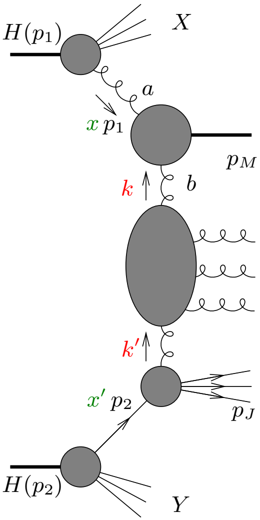

$$\frac{d\sigma}{dy_V\,d|p_{V\perp}|\,d\phi_V\,dy_J\,d|p_{J\perp}|\,d\phi_J} = \sum_{a,b}\int d^2k_\perp\,d^2k'_\perp$$

$$\times \int_0^1 dx\, f_a(x)\, V_{V,a}(k_\perp, x)$$

$$\times\, G(-k_\perp, -k'_\perp, \hat{s})$$

$$\times \int_0^1 dx'\, f_b(x')\, V_{J,b}(-k'_\perp, x'),$$

Master formula

$k_\perp$-factorization description of the process

$\hat{s} = x\, x'\, s$

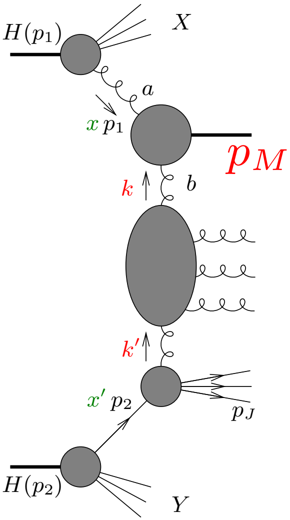

???

$$
\frac{d\sigma}{dy_V\, d|p_{V\perp}|\, d\phi_V\, dy_J\, d|p_{J\perp}|\, d\phi_J}
= \sum_{a,b} \int d^2k_\perp\, d^2k'_\perp
\times \int_0^1 dx\, f_a(x)\, V_{V,a}(k_\perp, x)
\times G(-k_\perp, -k'_\perp, \hat{s})
\times \int_0^1 dx'\, f_b(x')\, V_{J,b}(-k'_\perp, x'),
$$

The NRQCD formalism

Quarkonium production in NRQCD

- We first use the Non Relativistic QCD (NRQCD) formalism
  Bodwin, Braaten, Lepage; Cho, Leibovich ....
- Proof of NRQCD factorization: NLO Nayak Qiu Sterman 05; all orders Nayak 15.
- Expands the onium state wrt the velocity $v \sim \frac{1}{\log M}$ of its constituents:

$$|J/\psi\rangle = O(1)\left|Q\bar{Q}[^3S_1^{(1)}]\right\rangle + O(v)\left|Q\bar{Q}[^3P_J^{(8)}]g\right\rangle + O(v^2)\left|Q\bar{Q}[^1S_0^{(8)}]g\right\rangle +$$
$$+O(v^2)\left|Q\bar{Q}[^3S_1^{(1,8)}]gg\right\rangle + O(v^2)\left|Q\bar{Q}[^3D_J^{(1,8)}]gg\right\rangle + \ldots\ldots$$

  - all the non-perturbative physics is encoded in Long Distance Matrix Elements (LDME) obtained from $|J/\psi\rangle$
  - hard part (series in α_s): obtained by the usual Feynman diagram methods
  - the cross-sec. = convolution of (the hard part)^2 * LDME
- In NRQCD, the two Q and $\bar{Q}$ share the quarkonium momentum: $p_V = 2q$
- The relative importance of color-singlet versus color-octet mechanisms is still subject of discussions.
- We consider the case where the $Q\bar{Q}$-pair has the same spin and orbital momentum as the J/Ψ : $\left|Q\bar{Q}[^3S_1^{(1)}]\right\rangle$ and $\left|Q\bar{Q}[^3S_1^{(8)}]gg\right\rangle$ Fock states
- We treat the vertex V_V at LO

The J/ψ impact factor: NRQCD color singlet contribution

From open quark-antiquark gluon production to J/ψ production

NRQCD color-singlet transition vertex:

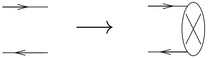

$$[v(q)\bar{u}(q)]^{ij}_{\alpha\beta} \to \frac{\delta^{ij}}{4N}\left(\frac{\langle \mathcal{O}_1\rangle_V}{m}\right)^{1/2}[\hat{\epsilon}^*_V\,(2\hat{q}+2m)]_{\alpha\beta}$$

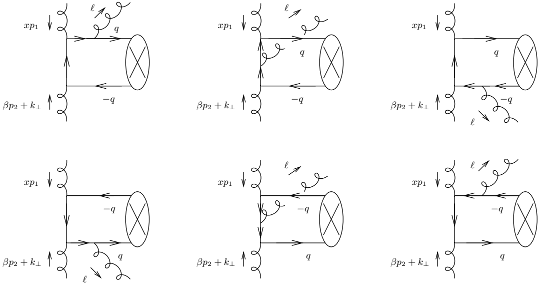

note the unobserved gluon due to C-parity conservation

$\langle \mathcal{O}_1\rangle_{J/\psi}$ from leptonic J/Ψ decay rate $\qquad \langle \mathcal{O}_1\rangle_{J/\psi} \in [0.387, 0.444]\ \mathrm{GeV}^3$

The J/ψ impact factor: NRQCD color octet contribution

From open quark-antiquark production to J/ψ production

NRQCD color-octet transition vertex: 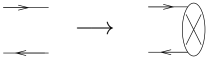

$$[v(q)\bar{u}(q)]^{ij\to d}_{\alpha\beta} \to t^d_{ij} d_8 \left(\frac{\langle \mathcal{O}_8 \rangle_V}{m}\right)^{1/2} [\hat{\epsilon}^*_V \, (2\hat{q} + 2m)]_{\alpha\beta}$$

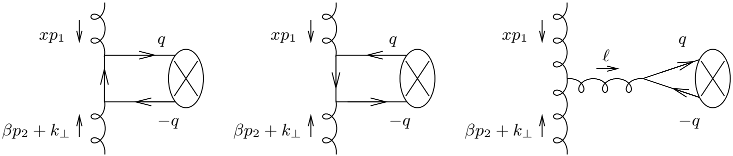

- the $Q\bar{Q}$ color-octet pair subsequently emits two soft gluons and turns into a $Q\bar{Q}$ color-singlet pair
- the $Q\bar{Q}$ color-singlet pair then hadronizes into a J/ψ.

$$\langle \mathcal{O}_8 \rangle_{J/\psi} \in [0.224 \times 10^{-2}, 1.1 \times 10^{-2}]\,\mathrm{GeV}^3$$

The Color Evaporation Model

Quarkonium production in the color evaporation model

Relies on the local duality hypothesis
Fritzsch, Halzen ...

Very crude approximation!

- Consider a heavy quark pair $Q\bar{Q}$ with $m_{Q\bar{Q}} < 2\,m_{Q\bar{q}}$
  $Q\bar{q}$ = lightest meson which contains Q
  e.g $D-$meson for $Q = c$
- it eventually produces a bound $Q\bar{Q}$ pair after a series of randomized soft interactions between its production and its confinement in $\frac{1}{9}$ cases, independently of its color and spin.
- It is assumed that the repartition between all the possible charmonium states is universal.
- Thus the procedure is the following :
  - Compute all the Feynman diagrams for open $Q\bar{Q}$ production
  - Sum over all spins and colors
  - Integrate over the $Q\bar{Q}$ invariant mass

The J/ψ impact factor: relying on the color evaporation model

From open quark-antiquark gluon production to J/ψ production

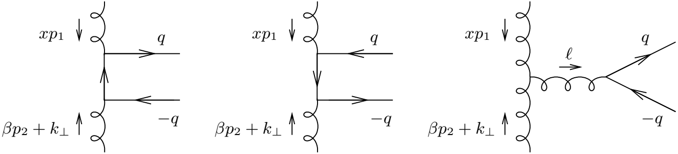

$$\sigma_{J/\psi} = F_{J/\psi} \int_{4m_c^2}^{4m_D^2} dM^2 \frac{d\sigma_{c\bar{c}}}{dM^2}$$

$F_{J/\psi}$: varied in [0.02, 0.04], poorly known

Numerical results

Kinematics and parameters

- Two center-of-mass energies: $\sqrt{s} = 8$ TeV and $\sqrt{s} = 13$ TeV
- Equal value of the transverse momenta of the J/ψ and the jet:
$$|p_{V\perp}| = |p_{J\perp}| = p_\perp$$
- Four different kinematic configurations:
  - CASTOR@CMS:
    - $0 < y_V < 2.5, \ -6.5 < y_J < -5, \ p_\perp = 10$ GeV
  - main detectors at ATLAS and CMS:
    - $0 < y_V < 2.5, \ -4.5 < y_J < 0, \ p_\perp = 10$ GeV
    - $0 < y_V < 2.5, \ -4.5 < y_J < 0, \ p_\perp = 20$ GeV
    - $0 < y_V < 2.5, \ -4.5 < y_J < 0, \ p_\perp = 30$ GeV
- Uncertainty bands:
  - variation of non-pert. constants
  - variation of scales μ_R, μ_F

Numerical results

Differential cross sections $\sqrt{s} = 8$ TeV

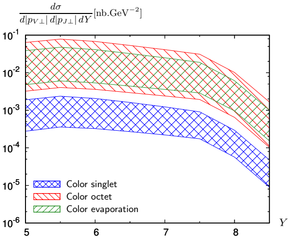

$0 < y_V < 2.5,\ -6.5 < y_J < -5,\ p_\perp = 10$ GeV

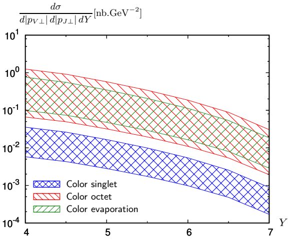

$0 < y_V < 2.5,\ -4.5 < y_J < 0,\ p_\perp = 10$ GeV

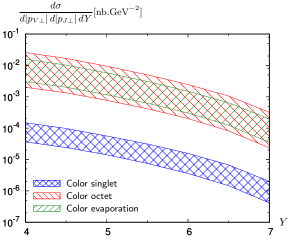

$0 < y_V < 2.5,\ -4.5 < y_J < 0,\ p_\perp = 20$ GeV

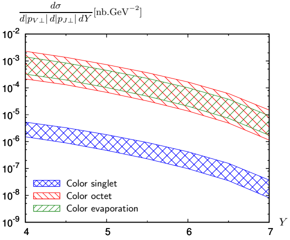

$0 < y_V < 2.5,\ -4.5 < y_J < 0,\ p_\perp = 30$ GeV

- color-octet dominates over color-singlet specially for large $p_\perp$
- color-octet and color-evaporation model give similar results

Numerical results

Differential cross sections $\sqrt{s} = 13$ TeV

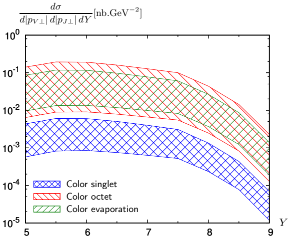

$0 < y_V < 2.5,\ -6.5 < y_J < -5,\ p_\perp = 10$ GeV

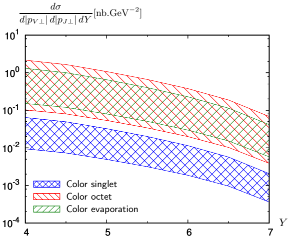

$0 < y_V < 2.5,\ -4.5 < y_J < 0,\ p_\perp = 10$ GeV

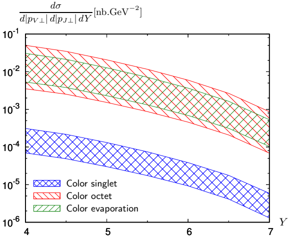

$0 < y_V < 2.5,\ -4.5 < y_J < 0,\ p_\perp = 20$ GeV

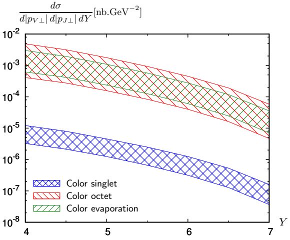

$0 < y_V < 2.5,\ -4.5 < y_J < 0,\ p_\perp = 30$ GeV

- color-octet dominates over color-singlet specially for large $p_\perp$
- color-octet and color-evaporation model give similar results
- slight increase of cross-sections when $\sqrt{s} = 8$ TeV $\rightarrow$ $\sqrt{s} = 13$ TeV

Numerical results

$\langle \cos \varphi \rangle$ $\sqrt{s} = 8$ TeV

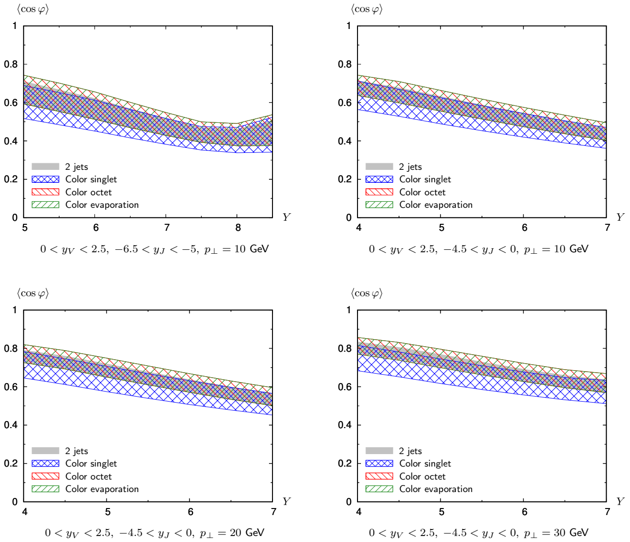

- all 3 models lead to similar decorrelation effects
- they are compatible with the case where $V_{J/\psi} \longrightarrow LO\, V_{jet}$

Numerical results

$\langle \cos \varphi \rangle$ $\sqrt{s} = 13$ TeV

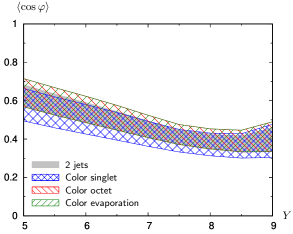

$0 < y_V < 2.5,\ -6.5 < y_J < -5,\ p_\perp = 10$ GeV

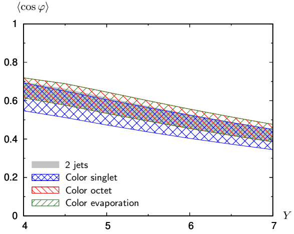

$0 < y_V < 2.5,\ -4.5 < y_J < 0,\ p_\perp = 10$ GeV

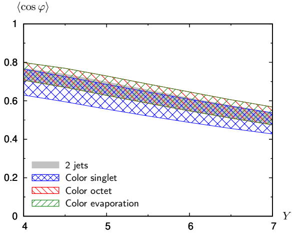

$0 < y_V < 2.5,\ -4.5 < y_J < 0,\ p_\perp = 20$ GeV

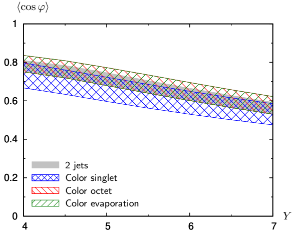

$0 < y_V < 2.5,\ -4.5 < y_J < 0,\ p_\perp = 30$ GeV

- all 3 models lead to similar decorrelation effects
- they are compatible with the case where $V_{J/\psi} \longrightarrow LO\ V_{jet}$
- slight increase of decorrelation effects when $\sqrt{s} = 8$ TeV $\rightarrow$ $\sqrt{s} = 13$ TeV

Factorized picture in the projectile frame

see G. Chirilli's talk

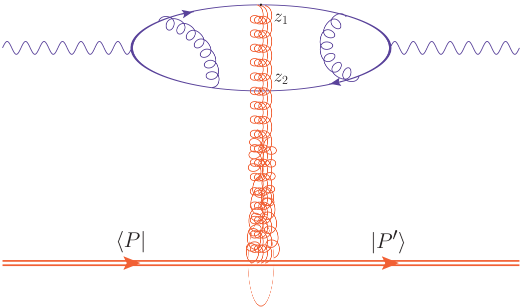

Factorized amplitude

$$\mathcal{A}^\eta = \int d^{D-2}\vec{z}_1 d^{D-2}\vec{z}_2 \, \Phi^\eta(\vec{z}_1, \vec{z}_2) \, \langle P'|[\mathrm{Tr}(U^\eta_{\vec{z}_1} U^{\eta\dagger}_{\vec{z}_2}) - N_c]|P\rangle$$

Dipole operator $\mathcal{U}^\eta_{ij} = \frac{1}{N_c}\mathrm{Tr}(U^\eta_{\vec{z}_i} U^{\eta\dagger}_{\vec{z}_j}) - 1$

Written similarly for any number of Wilson lines in any color representation!

Practical use of the formalism

- Compute the upper impact factor using the effective Feynman rules
- Build non-perturbative models for the matrix elements of the Wilson line operators acting on the target states
- Solve the B-JIMWLK evolution for these matrix elements with such non-perturbative initial conditions at a typical target rapidity $\eta = Y_0$.
- Evaluate the solution at a typical projectile rapidity $\eta = Y$, or at the rapidity of the slowest gluon
- Convolute the solution and the impact factor

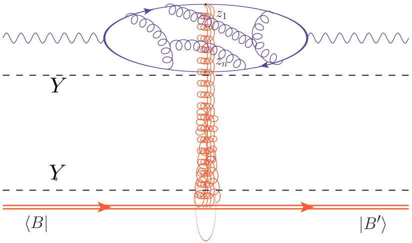

$$\mathcal{A} = \int d\vec{z}_1 ... d\vec{z}_n \; \Phi(\vec{z}_1, ..., \vec{z}_n) \times \langle P'| U_{\vec{z}_1} ... U_{\vec{z}_n} |P\rangle$$

Exclusive diffraction allows one to probe the $b_\perp$-dependence of the non-perturbative scattering amplitude

Exclusive dijet production

- Regge-Gribov limit : $s \gg Q^2 \gg \Lambda_{QCD}$
- Otherwise completely general kinematics
- Shockwave (CGC) Wilson line approach
- Transverse dimensional regularization $d = 2 + 2\varepsilon$, longitudinal cutoff

$$|p_g^+| > \alpha p_\gamma^+$$

LO diagram

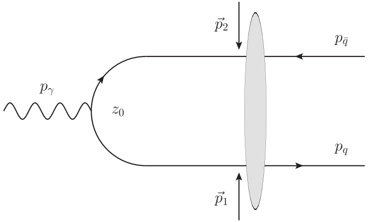

$$\mathcal{A} = \frac{\delta^{ik}}{\sqrt{N_c}} \int d^D z_0 [\bar{u}(p_q, z_0)]_{ij} (-ie_q) \hat{\varepsilon}_\gamma e^{-i(p_\gamma \cdot z_0)} [v(p_{\bar{q}}, z_0)]_{jk} \theta(-z_0^+)$$

$$= \delta(p_q^+ + p_{\bar{q}} - p_\gamma^+) \int d^d\vec{p}_1 d^d\vec{p}_2 \delta(\vec{p}_q + \vec{p}_{\bar{q}} - \vec{p}_\gamma - \vec{p}_1 - \vec{p}_2)\, \Phi_0(\vec{p}_1, \vec{p}_2)$$

$$\times C_F \left\langle P' \right| \tilde{\mathcal{U}}^\alpha(\vec{p}_1, \vec{p}_2) \left| P \right\rangle$$

$$\tilde{\mathcal{U}}^\alpha(\vec{p}_1, \vec{p}_2) = \int d^d\vec{z}_1 d^d\vec{z}_2\, e^{-i(\vec{p}_1\cdot\vec{z}_1) - i(\vec{p}_2\cdot\vec{z}_2)} [\tfrac{1}{N_c} \mathrm{Tr}(U^\alpha_{\vec{z}_1} U^{\alpha\dagger}_{\vec{z}_2}) - 1]$$

NLO open $q\bar{q}$ production

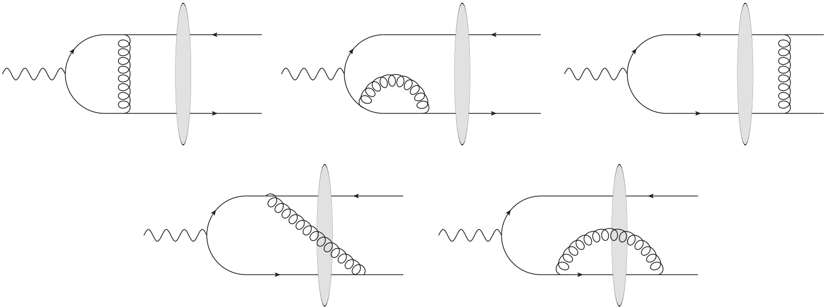

Diagrams contributing to the NLO correction

First kind of virtual corrections

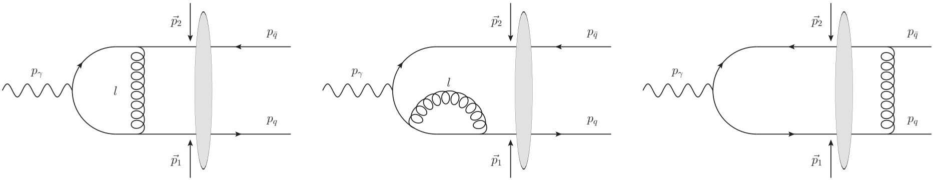

$$\mathcal{A}^{(1)}_{NLO} \propto \delta(p_q^+ + p_{\bar{q}} - p_\gamma^+) \int d^d\vec{p}_1 d^d\vec{p}_2 \delta(\vec{p}_q + \vec{p}_{\bar{q}} - \vec{p}_\gamma - \vec{p}_1 - \vec{p}_2)\, \Phi_{V1}(\vec{p}_1, \vec{p}_2\,)$$

$$\times C_F \left\langle P' \right| \tilde{\mathcal{U}}^\alpha(\vec{p}_1, \vec{p}_2) \left| P \right\rangle$$

Second kind of virtual corrections

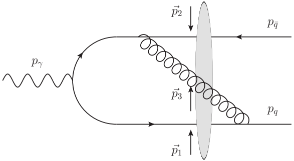

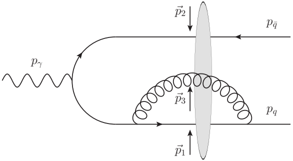

$$\mathcal{A}_{NLO}^{(2)} \propto \delta(p_q^+ + p_{\bar{q}} - p_\gamma^+) \int d^d\vec{p}_1 d^d\vec{p}_2 d^d\vec{p}_3 \delta(\vec{p}_q + \vec{p}_{\bar{q}} - \vec{p}_\gamma - \vec{p}_1 - \vec{p}_2 - \vec{p}_3)$$
$$\times [\Phi'_{V1}(\vec{p}_1, \vec{p}_2) C_F \left\langle P' \right| \tilde{\mathcal{U}}^\alpha(\vec{p}_1, \vec{p}_2) \left| P \right\rangle$$
$$+ \Phi_{V2}(\vec{p}_1, \vec{p}_2, \vec{p}_3) \left\langle P' \right| \tilde{\mathcal{W}}(\vec{p}_1, \vec{p}_2, \vec{p}_3) \left| P \right\rangle]$$

LO open $q\bar{q}g$ production

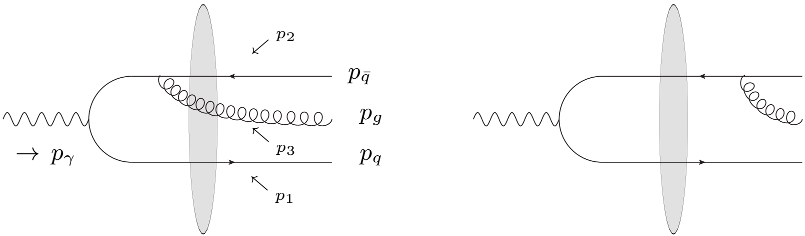

$$\mathcal{A}_R^{(2)} \propto \delta(p_q^+ + p_{\bar{q}} + p_g^+ - p_\gamma^+) \int d^d\vec{p}_1 d^d\vec{p}_2 d^d\vec{p}_3 \delta(\vec{p}_q + \vec{p}_{\bar{q}} + \vec{p}_g - \vec{p}_\gamma - \vec{p}_1 - \vec{p}_2 - \vec{p}_3)$$

$$\times [\Phi'_{R1}(\vec{p}_1, \vec{p}_2) C_F \left\langle P' \middle| \tilde{\mathcal{U}}^\alpha(\vec{p}_1, \vec{p}_2) \middle| P \right\rangle$$

$$+ \Phi_{R2}(\vec{p}_1, \vec{p}_2, \vec{p}_3) \left\langle P' \middle| \tilde{\mathcal{W}}(\vec{p}_1, \vec{p}_2, \vec{p}_3) \middle| P \right\rangle]$$

$$\mathcal{A}_R^{(1)} \propto \delta(p_q^+ + p_{\bar{q}} + p_g^+ - p_\gamma^+) \int d^d\vec{p}_1 d^d\vec{p}_2 \delta(\vec{p}_q + \vec{p}_{\bar{q}} + \vec{p}_g - \vec{p}_\gamma - \vec{p}_1 - \vec{p}_2)$$

$$\times \Phi_{R1}(\vec{p}_1, \vec{p}_2) C_F \left\langle P' \middle| \tilde{\mathcal{U}}^\alpha(\vec{p}_1, \vec{p}_2) \middle| P \right\rangle$$

Divergences

Divergences

- Rapidity divergence $p_g^+ \to 0$ $\Phi_{V2}\Phi_0^* + \Phi_0\Phi_{V2}^*$
- UV divergence $\vec{p}_g^{\,2} \to +\infty$ $\Phi_{V1}\Phi_0^* + \Phi_0\Phi_{V1}^*$
- Soft divergence $p_g \to 0$ $\Phi_{V1}\Phi_0^* + \Phi_0\Phi_{V1}^*, \Phi_{R1}\Phi_{R1}^*$
- Collinear divergence $p_g \propto p_q$ or $p_{\bar{q}}$ $\Phi_{R1}\Phi_{R1}^*$
- Soft and collinear divergence $p_g = \frac{p_g^+}{p_q^+}p_q$ or $\frac{p_g^+}{p_{\bar{q}}^+}p_{\bar{q}}$, $p_g^+ \to 0$ $\Phi_{R1}\Phi_{R1}^*$

Rapidity divergence

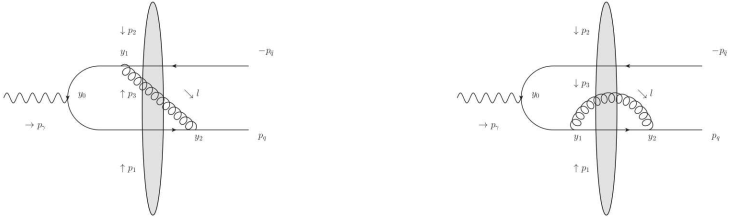

Double dipole virtual correction Φ_{V2}

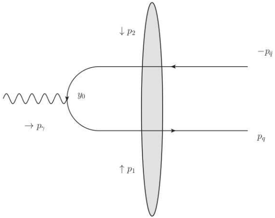

B-JIMWLK evolution of the LO term : $\Phi_0 \otimes \mathcal{K}_{BK}$

Rapidity divergence

B-JIMWLK equation for the dipole operator

$$\frac{\partial \tilde{\mathcal{U}}_{12}^{\alpha}}{\partial \log \alpha} = 2\alpha_s N_c \mu^{2-d} \int \frac{d^d\vec{k}_1 d^d\vec{k}_2 d^d\vec{k}_3}{(2\pi)^{2d}} \delta(\vec{k}_1 + \vec{k}_2 + \vec{k}_3 - \vec{p}_1 - \vec{p}_2) \left(\tilde{\mathcal{U}}_{13}^{\alpha}\tilde{\mathcal{U}}_{32}^{\alpha} + \tilde{\mathcal{U}}_{13}^{\alpha} + \tilde{\mathcal{U}}_{32}^{\alpha} - \tilde{\mathcal{U}}_{12}^{\alpha}\right)$$
$$\times \left[2\frac{(\vec{k}_1 - \vec{p}_1)\cdot(\vec{k}_2 - \vec{p}_2)}{(\vec{k}_1 - \vec{p}_1)^2(\vec{k}_2 - \vec{p}_2)^2} + \frac{\pi^{\frac{d}{2}}\Gamma(1-\frac{d}{2})\Gamma^2(\frac{d}{2})}{\Gamma(d-1)} \left(\frac{\delta(\vec{k}_2 - \vec{p}_2)}{\left[(\vec{k}_1 - \vec{p}_1)^2\right]^{1-\frac{d}{2}}} + \frac{\delta(\vec{k}_1 - \vec{p}_1)}{\left[(\vec{k}_2 - \vec{p}_2)^2\right]^{1-\frac{d}{2}}} \right) \right]$$

η rapidity divide, which separates the upper and the lower impact factors

$$\Phi_0 \tilde{\mathcal{U}}_{12}^{\alpha} \to \Phi_0 \tilde{\mathcal{U}}_{12}^{\eta} + 2\log\left(\frac{e^{\eta}}{\alpha}\right) \mathcal{K}_{BK} \Phi_0 \tilde{\mathcal{W}}_{123}$$

Provides a counterterm to the $log(\alpha)$ divergence in the virtual double dipole impact factor:

$\Phi_0 \tilde{\mathcal{U}}_{12}^{\alpha} + \Phi_{V2} \tilde{\mathcal{W}}_{123}^{\alpha}$ is finite and independent of α

Divergences

- Rapidity divergence
- UV divergence $\vec{p}_g^{\,2} \to +\infty$ $\Phi_{V1}\Phi_0^* + \Phi_0\Phi_{V1}^*$
- Soft divergence $p_g \to 0$ $\Phi_{V1}\Phi_0^* + \Phi_0\Phi_{V1}^*, \Phi_{R1}\Phi_{R1}^*$
- Collinear divergence $p_g \propto p_q$ or $p_{\bar{q}}$ $\Phi_{R1}\Phi_{R1}^*$
- Soft and collinear divergence $p_g = \frac{p_g^+}{p_q^+}p_q$ or $\frac{p_g^+}{p_{\bar{q}}^+}p_{\bar{q}}$, $p_g^+ \to 0$ $\Phi_{R1}\Phi_{R1}^*$

UV divergence

Dressing of the external lines

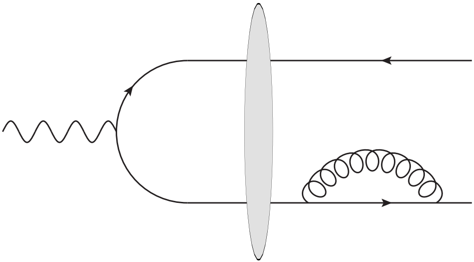

Some null diagrams just contribute to turning UV divergences into IR divergences

$$\Phi = 0 \propto \left(\frac{1}{2\epsilon_{IR}} - \frac{1}{2\epsilon_{UV}} \right)$$

Divergences

- Rapidity divergence
- UV divergence
- Soft divergence $p_g \to 0$ $\Phi_{V1}\Phi_0^* + \Phi_0\Phi_{V1}^*$, $\Phi_{R1}\Phi_{R1}^*$
- Collinear divergence $p_g \propto p_q$ or $p_{\bar{q}}$ $\Phi_{R1}\Phi_{R1}^*$
- Soft and collinear divergence $p_g = \frac{p_g^+}{p_q^+}p_q$ or $\frac{p_g^+}{p_{\bar{q}}^+}p_{\bar{q}}$, $p_g^+ \to 0$ $\Phi_{R1}\Phi_{R1}^*$

Soft and collinear divergence

Jet cone algorithm

We define a cone width for each pair of particles with momenta p_i and p_k, rapidity difference ΔY_{ik} and relative azimuthal angle $\Delta\varphi_{ik}$

$$(\Delta Y_{ik})^2 + (\Delta\varphi_{ik})^2 = R_{ik}^2$$

If $R_{ik}^2 < R^2$, then the two particles together define a single jet of momentum $p_i + p_k$.

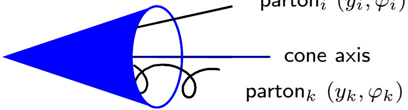

Applying this in the small R^2 limit cancels our soft and collinear divergence.

Divergences

- Rapidity divergence
- UV divergence
- Soft divergence $p_g \to 0$ $\Phi_{V1}\Phi_0^* + \Phi_0\Phi_{V1}^*, \Phi_{R1}\Phi_{R1}^*$
- Collinear divergence $p_g \propto p_q$ or $p_{\bar{q}}$ $\Phi_{R1}\Phi_{R1}^*$
- Soft and collinear divergence

The remaining divergences cancel the standard way:
virtual corrections and real corrections cancel each other

Phenomenological applications

- diffractive exclusive dijet production is a key observable: it gives an access to the Wigner dipole function Y. Hatta, B-W. Xiao, F. Yuan
- a ZEUS diffractive exclusive dijet measurements was performed, and the azimuthal distribution of the two jets was obtained
  - this relies on an exclusive algorithm, in which a y parameter regularize both soft and collinear singularities
  - using a small y limit, and for large β, there is a good agreement with a Golec-Biernat Wüsthoff model combined with our NLO impact factor

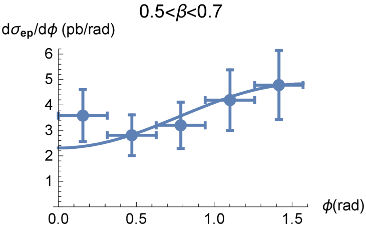

$$\beta = \frac{Q^2}{Q^2 + M^2_{\rm dijet} - t}$$

  - within ZEUS kinematical cuts, the linear BFKL regime dominates
- our agreement is a good sign that perturbative Regge-like description are favored with respect to collinear type descriptions
- EIC should give a direct access to the saturated region
- a complete description of ZEUS data, in the whole β-range, requires to go beyond the small y approximation

The ultimate picture

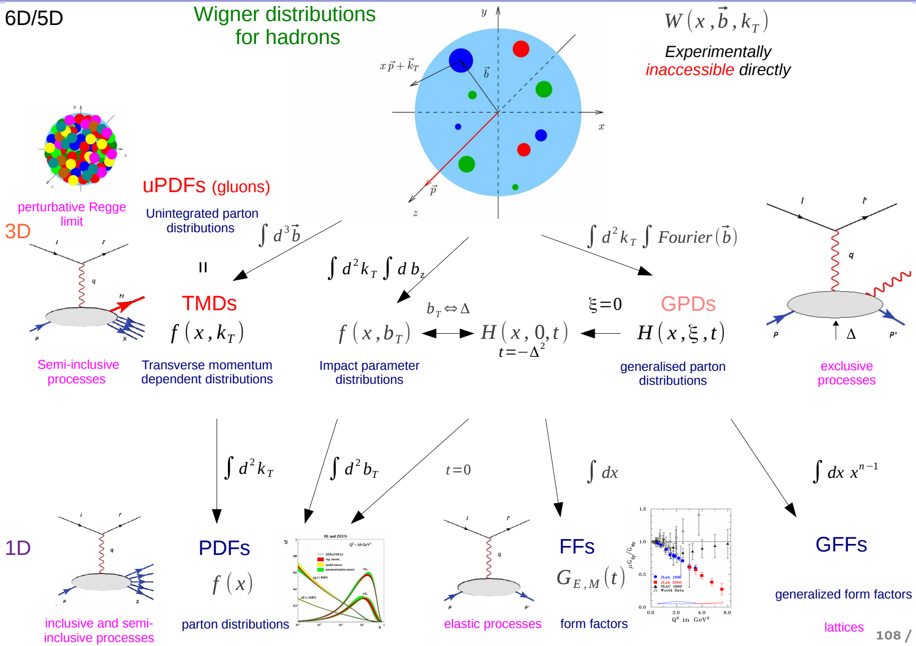

Comparison: 13 TeV vs. 7 TeV

Azimuthal correlation $\langle \cos\varphi \rangle$

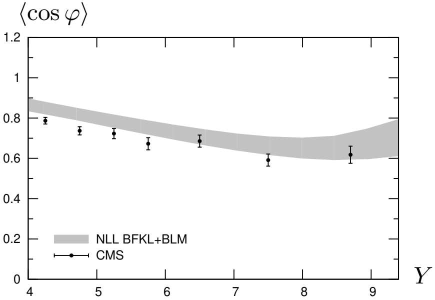

$\sqrt{s} = 7$ TeV

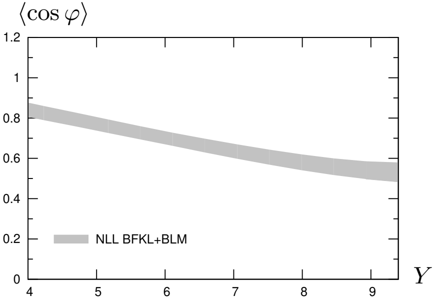

$\sqrt{s} = 13$ TeV

The behavior is similar at 13 TeV and at 7 TeV

Comparison: 13 TeV vs. 7 TeV

Azimuthal distribution (integrated over $6 < Y < 9.4$)

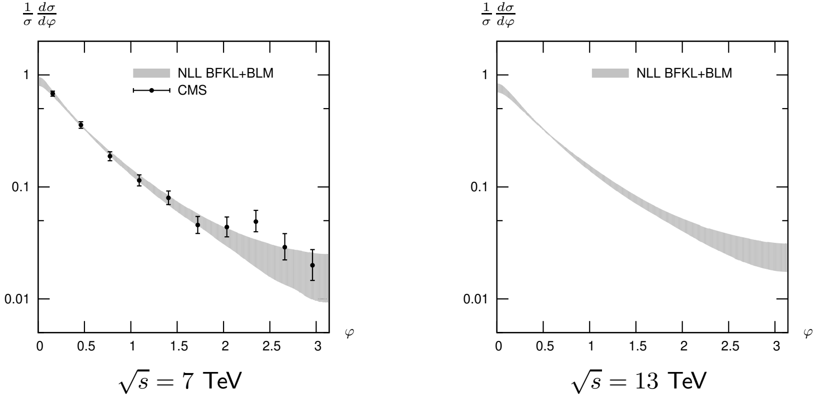

The behavior is similar at 13 TeV and at 7 TeV

Comparison: 13 TeV vs. 7 TeV

Azimuthal correlation $\langle \cos 2\varphi \rangle / \langle \cos \varphi \rangle$

(asymmetric configuration)

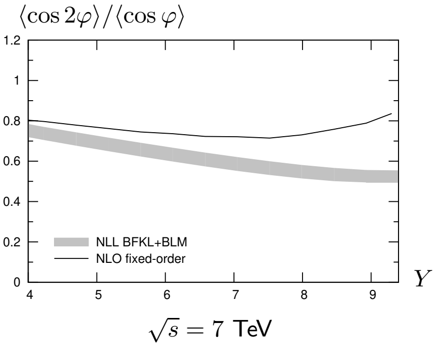

The difference between BFKL and fixed-order is smaller at 13 TeV than at 7 TeV

Numerical implementation

In practice: two codes have been developed

A *Mathematica* code, exploratory

D. Colferai, F. Schwennsen, L. Szymanowski, S. W.
JHEP 1012:026 (2010) 1-72 [arXiv:1002.1365 [hep-ph]]

- jet cone-algorithm with $R = 0.5$
- MSTW 2008 PDFs (available as *Mathematica* packages)
- $\mu_R = \mu_F$ (in MSTW 2008 PDFs); we take $\mu_R = \mu_F = \sqrt{|\mathbf{k}_{J1}|\,|\mathbf{k}_{J2}|}$
- two-loop running coupling $\alpha_s(\mu_R^2)$
- we use a ν grid (with a dense sampling around 0)
- we use Cuba integration routines (in practice Vegas): precision 10^{-2} for 500.000 max points per integration
- mapping $|\mathbf{k}| = |\mathbf{k}_J| \tan(\xi\pi/2)$ for $\mathbf{k}$ integrations $\Rightarrow [0,\infty[\to [0,1]$
- although formally the results should be finite, it requires a special grouping of the integrand in order to get stable results
  $\Longrightarrow$ 14 minimal stable basic blocks to be evaluated numerically
- rather slow code

Numerical implementation

A *Fortran* code, $\simeq 20$ times faster

B. Ducloué, L. Szymanowski, S.W.
JHEP 05 (2013) 096 [arXiv:1207.7012 [hep-ph]]

- Check of our *Mathematica* based results
- Detailled check of previous mixed studies (NLL Green's function + LL jet vertices)
- Allows for k_J integration in a finite range
- Stability studies (PDFs, etc...) made easier
- Comparison with the recent small R study of D. Yu. Ivanov, A. Papa
- Azimuthal distribution
- More detailled comparison with fixed order NLO:
  there is a hope to distinguish NLL BFKL / NLO fixed order
- Problems remain with ν integration for low Y
  (for $Y < \frac{\pi}{2\alpha_s N_c} \sim 4$). To be fixed!

  We restrict ourselves to $Y > 4$.

Integration over $|\mathbf{k}_J|$

Experimental data is integrated over some range, $k_{J\mathrm{min}} \leq k_J = |\mathbf{k}_J|$

Growth of the cross section with increasing $k_{J\mathrm{max}}$:

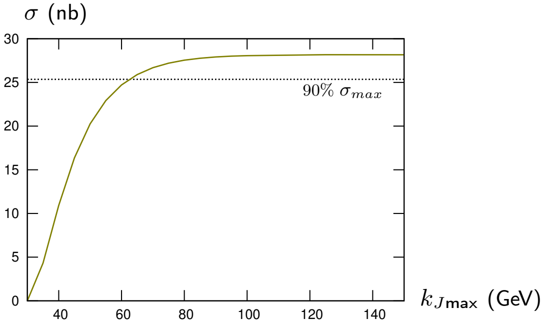

$\Rightarrow$ need to integrate up to $k_{J\mathrm{max}} \sim 60$ GeV

A consistency check of stability of $|\mathbf{k}_J|$ integration have been made:

- consider the simplified NLL Green's function + LL jet vertices scenario
- the integration $\int_{k_{J\,min}}^{\infty} dk_J$ can be performed analytically
- comparison with integrated results of Sabio Vera, Schwennsen is safe